ASYNCHRONOUS PROCESSING OF LUMINANCE DIFFERENCE AND MOTION IN VISUAL PERCEPTION

by

Onur İşcan

B.S. in Physics Engineering, Faculty of Science and Letters,
İstanbul Technical University, 2005

Submitted to the Institute of Biomedical Engineering
in partial fulfillment of the requirements
for the degree of
Master of Science
in
Biomedical Engineering

Boğaziçi University
June, 2008

ASYNCHRONOUS PROCESSING OF LUMINANCE DIFFERENCE AND MOTION IN VISUAL PERCEPTION

APPROVED BY:

Assist. Prof. Dr. Burak Güçlü (Thesis Advisor)	……
Assist. Prof. Dr. Murat Gülsoy	……...
Prof. Dr. Reşit Canbeyli	……

DATE OF APPROVAL:

ACKNOWLEDGEMENTS

I would like to thank my advisor Assist. Prof. Dr. Burak Güçlü for his support, guidance, patience and contribution at every step of this study.

I would also like to thank Prof. Dr. Haluk Öğmen and Prof. Dr. Bart Farell for their interest and support.

Lastly, I would like to thank my subjects, family and friends, for their support, tolerance and patience.

ABSTRACT

ASYNCHRONOUS PROCESSING OF LUMINANCE DIFFERENCE AND MOTION IN VISUAL PERCEPTION

Motion perception is classified into the perception of first-order and second-order motion. First-order motion is a luminance defined one that occurs when differences in mean luminance between two adjacent areas of an image are displaced. On the other hand, second-order motion is motion in which the moving contour is defined by contrast, texture or flicker. This study is related with the perception of first-order motion. The processing of visual information in the human brain is accomplished by numerous visual streams. Each stream is specialized to process different attributes of the visual scene. Two of the well-known streams are the parvocellular and magnocellular pathways. Both the detection of luminance change and the perception of motion are assumed to be functions of the magnocellular stream and the associated parietal areas in the visual cortex because of the fast response characteristics of the magnocellular stream and its high contrast sensitivity. It was already demonstrated that times-to-consciousness of form, color, luminance and motion differ. In the present study, it was investigated whether luminance difference and motion are perceived synchronously. The hypothesis was tested by modifying a particular task in the literature. The stimuli were filled squares presented on a mid-gray background. The luminance of the stimulus was continuously incremented or decremented and the subjects performed a lightness matching task based on the perceived luminance at motion instant. It was hypothesized that if the subjects perceived motion first, they would report luminance values back in time from the instant the motion had occurred. Significant main effects were found due to luminance at motion instant and luminance-change direction. When the luminance-change direction was from dim to bright, the matching errors decreased as a function of luminance at motion instant. On the other hand, when the luminance-change direction was from bright to dim, the matching errors increased as the luminance at motion instant increased. In both cases the reported luminance values at motion instant were biased towards the luminance-change direction. This suggested that motion was perceived later than luminance difference. A computational model was used to

predict the results of the current experiment. It was inspired by Reichardt type models which consist of luminance and motion detector channels. However, experimental results were not consistent with either the model prediction or the experimental results reported in the literature. This inconsistency may be due to a memory effect.

Keywords: luminance-motion asynchrony, luminance judgment, modular perception, visual memory, computational model

ÖZET

GÖRSEL ALGIDA PARLAKLIK FARKI VE HAREKETİN EŞZAMANSIZ İŞLENMESİ

Hareket algısı birinci ve ikinci mertebeden olmak üzere ikiye ayrılır. Birinci mertebeden hareket, parlaklık algısı temeline dayanır ve görüntüde iki komşu bölge arasındaki ortalama parlaklık farkının yer değiştirmesiyle oluşur. İkinci mertebeden hareket ise, hareketli şeklin kontrast, yüzey yapısı, titreşim gibi nitelikleriyle tanımlanan hareket türüdür. Bu çalışma, kullanılan yöntemler bakımından birinci dereceden hareket algısı üzerinedir. Görsel bilgi, insan beyninde birçok yoldan işlenir. Her akış yolu görüntünün farklı özelliklerinin işlenmesi için özelleşmiştir. Bu yollardan en çok bilinenler, magnoselular ve parvoselular akış yollarıdır. Hem parlaklık farkı algısı hem de hareket algısı magnoselular akışın işlevleri olarak kabul edilir ve magnoselular akışın hızlı yanıt özelliği ve yüksek kontrast hassasiyetinden ötürü görme korteksinin paryetal bölgesiyle ilişkilendirilir. Şekil, renk, parlaklık ve hareketin algılanma sürelerinin farklı olduğu önceki çalışmalarda gösterilmiştir. Bu çalışmada, parlaklık farkı ve hareket algılarının eşzamanlı olup olmadıkları incelenmiştir. Hipotez, literatürdeki bir yöntemden esinlenerek test edilmiştir. Uyarılar orta grilikteki arka plan üzerine içi dolu kareler olarak hazırlanmıştır. Deneylerde uyarının parlaklığı sürekli olarak artmakta veya azalmaktayken hareketin algılandığı andaki parlaklık algısı ölçüldü. Deneklerin hareketi önce algılamaları durumunda, hareketin olduğu andaki parlaklıktan önceki değerleri bildirmeleri beklenmekteydi. İstatistiksel anlamlı ana etkiler olarak hareket anındaki parlaklık ve parlaklık değişim yönü bulunmuştur. Parlaklık değişim yönü koyudan açığa doğruyken eşleştirme hataları hareket anındaki parlaklığa bağlı olarak azalmaktadır. Buna karşın, parlaklık değişim yönü açıktan koyuya doğruyken eşleştirme hataları hareket anındaki parlaklığa bağlı olarak artmaktadır. Her iki durumda da bildirilen hareket anındaki parlaklık değerleri parlaklık değişim yönünde bir eğilim göstermiştir. Bu durum, hareketin parlaklık farkından sonra algılandığını öne sürmektedir. Deneyin sonuçlarını karşılaştırmak

için hesaplamalı bir model kullanılmıştır. Model, parlaklık ve hareket detektörkanallarından oluşan Reichardt tipi bir modeli temel almıştır. Deneysel sonuçlar ne literatürdeki deneysel sonuçlarla ne de model tahminiyle örtüşmektedir. Bu uyuşmazlık bir bellek etkisinden kaynaklanıyor olabilir.

Anahtar kelimeler: parlaklık-hareket eşzamansızlığı, parlaklık kararı, modüler algı, görsel bellek, hesaplamalı model

TABLE OF CONTENTS

LIST OF FIGURES

LIST OF TABLES

LIST OF ABBREVIATIONS

P	Parvocellular
M	Magnocellular
K	Koniocellular
LGN	Lateral Geniculate Nucleus
MT	Middle Temporal Lobe
MAE	Motion After-Effect

1. INTRODUCTION

1.1 Objective

The visual brain is known to consist of many distinct visual areas, specialized to process and perceive different attributes of the visual scene. These attributes can be shape, form, color, luminance and motion. Different attributes are not perceived simultaneously. Instead some attributes are perceived before others. It was previously demonstrated that form, color and motion perceptions are asynchronous. Form and color are perceived before motion [1]. Since perceiving an attribute is being conscious of it, and perception of these different attributes is the result of activity in geographically distinct visual areas, it follows that visual consciousness is distributed in space. Equally, since different attributes were perceived at different times, visual consciousness is also distributed in time. Therefore, it follows that there is not a single unified visual consciousness, but there are instead many visual consciousnesses. Moreover, binding of activity in these different areas occurs post-consciously [1].

This study is on the perception of luminance difference and motion and to test if they are synchronous or dissociable events and perceived asynchronously. Motion perception is classified into two categories as first-order motion and second-order motion. First-order motion is the basis of this study. It is the motion that is due to the mean luminance difference between two adjacent areas on an image. Both motion and luminance difference perceptions are the functions of magnocellular pathway. This pathway has a fast response and high contrast sensitivity. Because of these characteristics, perception of motion and luminance difference may expected to be synchronous.

One of the previous studies, however, claims that motion is indeed perceived before luminance difference [2]. In Kerzel's experiment, the method was related to the perception time. The observer pursued a moving target. At some point during the pursuit, a flash was presented and the observer was asked to localize the target position at the time of the flash. The distance between true and judged eye position at flash presentation divided by the velocity of the eye movement gives the time-to-consciousness of the flash. The observers

were presented with a small object rotating around a central stationary point. At an unpredictable position, the luminance of the rotating object was changed. That is, the luminance difference between target and background which was continuously displaced on a circular trajectory was changed. The results showed that, target motion reached consciousness earlier than the luminance change. The target moved away from the true onset of the luminance change before the change reached awareness. The luminance change was mislocalized in the direction of motion. This indicated that motion was perceived before the luminance difference [2].

The hypothesis of this study is to test this claim by using an alternative method and different of stimuli. In this study, the same hypothesis is tested by reversing the task. The luminance of the stimulus was continuously incremented or decremented. The subjects responded according to the movement of the stimulus. It is hypothesized that if the subjects report a previous luminance value in the series at the motion instant, the motion must be processed first.

2. BACKGROUND

2.1 Anatomy and Physiology of the Eye

The eye may be thought of as consisting of three different layers. Figure 2.1 shows a horizontal cross section of the human eye. The outermost layer is the sclera, the middle layer is the uvea, and the innermost layer is the retina. The sclera is the white portion of the eye which is apparent on gross observation. This layer consists largely of collagen. It provides support and protection for the internal elements of the eye. The sclera is continuous with the cornea, which is the transparent tissue at the most anterior aspect of the eye. The most anterior aspect of the eye is the cornea. The cornea is a five-layered transparent structure. Approximately two thirds of the refractive power of the eye is provided by the cornea. The uvea is a highly vascularized tissue which, among other functions, plays a large role in providing nutrition to the various elements of the eye. The uvea is divided into three components: the iris, the ciliary body, and the choroid. The iris constricts in response to light and dilates in the absence of light. By controlling the diameter of the pupil, the iris helps to regulate the amount of light that enters the eye. The ciliary body has two primary functions. First, it contains a muscle, the ciliary muscle, that focuses the lens for near vision. This process is referred to as accomodation [3]. Second, the ciliary body is the source of the aqueous humor. The aqueous humor provides nourishment to the internal eye structures, including the cornea and the lens. The aqueous humor is contained within the anterior chamber of the eye. This fluid is continuously produced by the ciliary body and drained by the canal of Schlemm. The canal of Schlemm is located in the angle of the eye, where the iris inserts into the ciliary body. This structure runs circumferentially around the eye. Posterior to the anterior chamber is the crystalline lens. The lens provides about one third of the dioptric power of the eye. When viewing a distant object, the lens power is approximately 20 diopters. When viewing a near object, the dioptric power of the lens increases, thus allowing near objects to be clearly viewed. The vitreous humor makes up the bulk of the eye volume. It consists largely of collagen and hyaluronic acid and has a gel-like structure. The vitreous provides structural and nutritive support to the retina in additon to creating a dioptrically critical space. The choroid forms the bulk of the uveal track. The choroid serves the important role of

providing blood to the outermost aspects of the retina.The retina is the innermost tissue layer of the eye. It is exceedingly complex, multilayered neural element. The preceding optical elements foucs images on the retina. The retina then begins the complex task of analyzing these images [3].

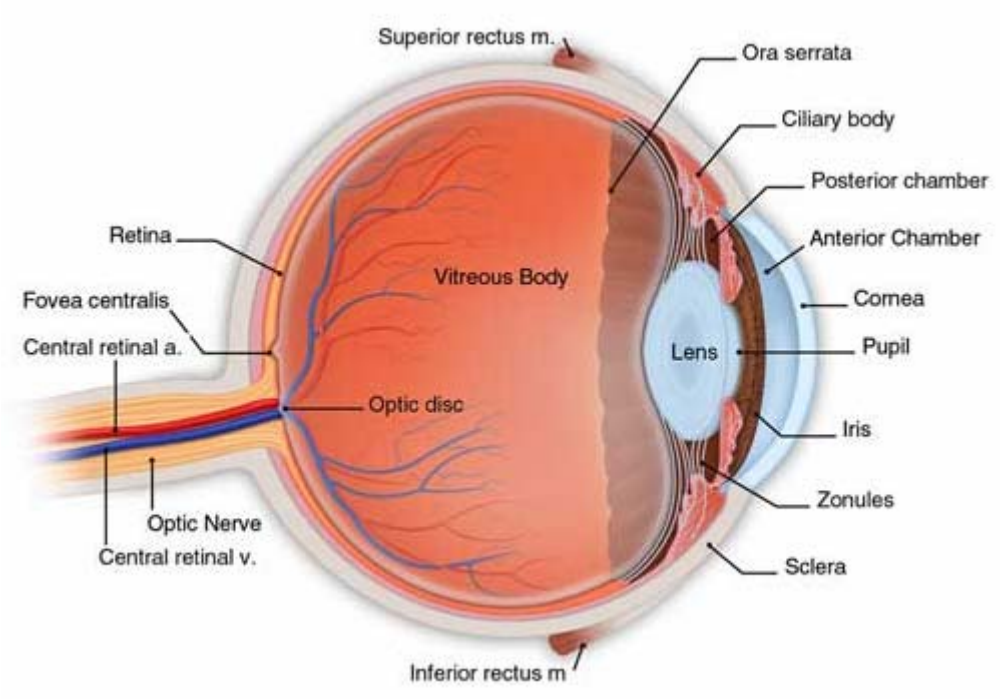

Figure 2.1 Anatomy of the eye [4].

2.2 Retina

Retina is the light sensitive part of the eye. Figure 2.2 shows cross sections of the primate retina. There are two types of receptors; these are the rods and cons. It is like a dual organ that has two networks. The rods are sensitive to weak light and have maximum sensitivity at about 507 nm whereas the cones are sensitive to strong light and have maximum sensitivity at 555 nm. Rod vision is called scotopic (dark-seeing) and cone vision is called photopic (light-seeing). Rods are located in all parts of the retina and being very sensitive to motion they give no color discrimination. Where cones are located in a small area is called the fovea, which is a shallow pit that is about 1.5 mm in diameter. Cone density decreases as it moves away from the fovea. The color vision is due to the cones and fovea lacks blood vessels and is acute. Macula Lutea is a pigmented part which surrounds the fovea. It's the yellow spot that contains a yellow dye, xanthrophyll, which absorbs ranges in wavelength from about 380 to 700 nm. Like larger blood vessels, nerves from the rest of the retina go around it [5].

In an average human retina there are 6-7 millions of cones, 110 to 130 millions of rods, but only 800.000 fibers in the optic nerve [5]. The connections are not simple because of the huge amounts of information sent to the brain. The optic nerves cross at the optic chiasma, where all the signals from the right side of the two retinas are sent to the right side of the brain and all the signals from the left are sent to the left side. These two halves of the picture are sent separately to each half of the brain. This way it is made sure that the loss of an eye does not affect the visual system. Halfway back through the brain the signals get distributed to the occipital (visual) cortex, which has the topology similar to the retina and it is the first stage of perception. There are several layers of nerve cells in the retina; horizontal, bipolar, amacrine and ganglion cells. Receptors synapse in the outer plexiform layer with horizontal cells and also the bipolar cells, and bipolars synapse in the inner plexiform layer with both amacrine and ganglion cells. Some ganglion cells get input directly, some receive it only via amacrines. The axons of the ganglion cells pass through the surface of the retina to the blindspot. Here they are bunched into the optic nerve that leads to the brain [5].

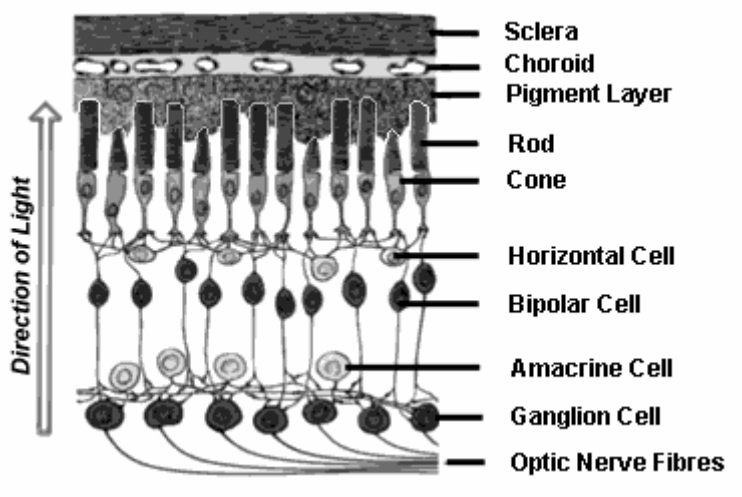

Figure 2.2 Retina [6].

2.3 Parvocellular - Magnocellular Cells

The retinal ganglion cells are two different types. One kind shows color-opponency and the other lacks color-opponency. The kind that shows the property of color opponency has the receptive fields that have antagonistic center and surround regions, and that the peak sensitivities of the two regions are at different wavelengths. On the other hand the other kind of ganglion cells has these regions at the same wavelength. These second type of cells respond a little to monochromatic light, but strongly to the difference in luminance between center and surround across a broad band of wavelengths. These two types of cells are most commonly called parvocellular (P) and magnocellular (M) cells. They could also be called color-opponent and broad-band because of the different responses to color stimuli. P and M come from the connection they make with parvocellular and magnocellular layers of the lateral geniculate nucleus (LGN) in the brain.

Parvocellular and magnocellular cells have some differences. First of all when we look at the response they give to stimulus; P cells give out a tonic (sustained) response. They keep on firing impulses. But M cells give a phasic (transient) response which is more rapid if the stimulus does not change. Second difference is, M cells have thicker axons compared to P cells, and therefore they conduct impulses quicker. Third is in the size of the

receptive field centers. M cells receptive fields are larger than those of P cells. M cells have 10 times lower contrast threshold than P cells. This lower contrast threshold could also mean that M cells have much higher contrast sensitivity, but there are fewer of them.

The main types of retinal ganglion cells are parvocellular and magnocellular cells but not all cells are a part of these two groups. Some of the cells have no concentric receptive fields, others have color- opponent responses without a concentric receptive field. These types form a third group of retinal ganglion cells that are also known as the koniocellular (K) pathway. In the retina the signals from neighboring receptors are grouped by horizontal cells. They form a receptive field of different/differing responses in the center and on the periphery, so that a uniform illumination of the field results in no net stimulus, but a difference in illumination of the center and periphery does. Some receptive fields use color differences like red-green/yellow-blue. Variations of stimuli are applied to color as well as brightness. There is more grouping in the lateral geniculate bodies and the visual cortex of receptive field for directional edge detection and eye dominance. This is low level processing prior to the high level interpretation. However this plays the role of difference in the senses, which is the basic of contrast phenomena. When retina is illuminated evenly in brightness and color, nerve activity is very little. The retina is a series of filters that run on the optic array. Optical formation of a retinal image and the pooling of light across each receptor aperture both work as low-pass spatial filters, and the probabilistic nature of the photon capture means a low-pass temporal filter, that can be critical at low light intensities. These early filters are then followed by the neural circuits of the retina, which in general act as high-pass temporal and spatial filters, though the processes of adaptation and lateral inhibition (centre-surround antagonism). The spatial summation of light responses within receptive field centers is another low-pass process, similar to the blurring forced by the optical filtering in the eye [7].

2.4 Motion Perception

Cornea focuses the light that enters the eye. Then the light passes through the iris, is further more focused by the lens. It hits the light-sensitive receptors of the retina at the back of the eye. Neural responses go through a series of linking cells. These cells are bipolar, horizontal and amacrine cells. The purpose of these cells is to combine and compare the responses from each photoreceptor before passing the signals onto the retinal ganglia cells. The links between cells provide a method for lateral inhibition; as a result the response of a cell becomes decreased by a large response in neighboring cells. This method is not absolute, it is only relative and it emphasizes the edges, and changes in the visual field and judgment of intensity.

As mentioned before, the visual system has two different pathways: The magnocellular and the parvocellular pathways. The magnocellular pathway identifies objects and their boundaries, as well as providing a basis for the understanding of depth and motion. This pathway begins in the retinal ganglion cell section with large receptive fields and it gets input from the achromatic opponent channel. The second pathway, the parvocellular pathway, is responsible for color and the details. This one gets input from all three color channels. They work independently and the judgments of each are made compatible afterwards in visual processing. Human visual pathway is shown in Figure 2.3.

The neural responses pass through the optic chiasm where the responses of the visual hemi-fields are sent to the opposite sides of the brain and to LGN which is located deep, on the side of the brain, from each sides of the visual field. Each LGN (one for each side of the brain) is divided into six layers. Two of these layers belong to the magnocellular pathway and the remaining four belong to the parvocellular pathway. Magnocellular pathway layers each receive input from the achromatic opponent channel that originates in one retina. The LGN also receives approximately 60% of the input from the visual pathways in the cortex at later stages. These upstream connections seem to offer a mechanism for expectations and previous perception to affect even the early stages of visual processing. These visual signals then proceed to the primary visual cortex also called the visual area 2 and then to higher visual processing areas.

The magnocellular pathway marks the boundaries and the locations of the objects. This pathway includes the achromatic opponent color channel, the magnocellular layers of the LGN, layers 4Ca and 4B of the primary visual cortex, the stripes in visual area 2 responsible for stereo and form perception, the middle temporal lobe (MT), and possibly the parieto-occipital region which is in charge of tasks involving the positions of objects. This pathway disregards the difference in the wavelength. It only considers the brightness difference during judgment. It has larger receptive fields compared to the parvocellular pathway. Not only are the responses faster, they are also transient and only small differences of contrast are needed for discrimination.

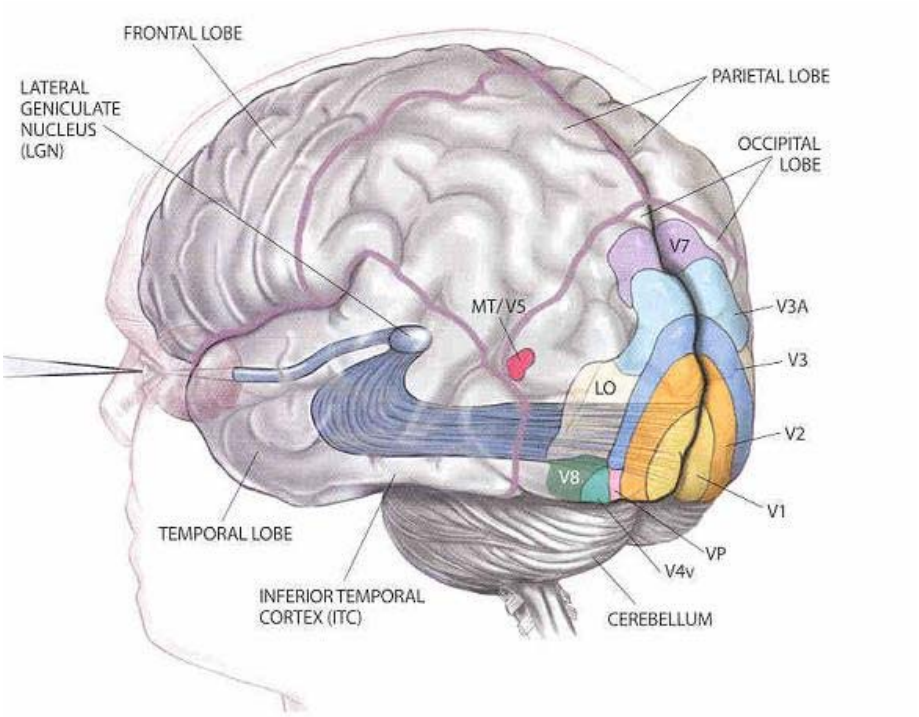

Figure 2.3 Human Visual Pathway. **V1:** Primary Visual Cortex begins processing of color, motion and shape. Cells in this area have the smallest receptive fields. **V2, V3, VP:** Continue processing cells; cells of each area have progressively larger receptive fields. **V3A:** Biased for perceiving motion. **V4v:** Function unknown. **MT/V5:** Detects motion. **V7:** Function unknown**. V8:** Processes color vision. **LO:** Plays a role in recognizing large-scale objects (*Scientific American*).

At the later stages of magnocellular pathway mainly in MT, there is a large number of cells that are selective to movement and direction signifying that it is also in charge of motion perception. Motion sensitive cells react to strong stimuli which are moving across their receptive field. Furthermore these cells are selective when it comes to direction and velocity of the motion. This works independently of other visual pathways; there a few people who have no perception of motion but have otherwise normal vision. Motion makes pattern vision possible by making sure that the stimulus of the retina is constantly changing. Motion helps us to know where to direct our eye movements, the time to impact with objects, and information about the site of parts of our body relative to other objects (exproprioceptive information) by giving us important hints to our relationship with our environment. Motion also supplies the information for the following: the relative depth, 3D structure, and grouping of objections.

Judgments made mainly by the magnocellular pathway, those of object boundaries, stereopsis, or motion; break down under conditions with no brightness differences between objects. Objects varying only in hue and saturation, not in brightness is a condition called equiluminance. The visual relationships that do not work under equiluminance are perspective depth cues, depth cues from relative motion, linking by common movement or collinearity, illusory borders, and illusions of size [8].

2.5 First-Order & Second-Order Motion

Motion perception is classified into two groups. We have both luminance-defined and contrast-defined information in our visual world. First-order motion perception is the perception of the motion of an object that differs in luminance from its background whereas second-order motion perception is the motion in which the moving stimulus is defined by modulating contrast over a textured area. There are strong differences between these two groups. First-order motion perception is described by a low-level motion detectors that consist of filters oriented in space and time (Adelson and Bergen, 1985; van Santen and Sperling, 1985; Watson and Ahumada, 1985). The detection of motion is done by detecting a change in luminance at one point on the retina after a delay. These kind of sensors are called Reichardt detectors, motion-energy sensors or Elaborated Reichardt

Detectors [9]. However, motion can be given by second-order properties lacking moving luminance cues. There are important perceptual differences between the two stimulus types. Prolonged viewing of unidirectional, luminance-based motion gives rise to a subsequent motion after-effect (MAE), in which physically stationary patterns will appear to move. Thus, theoretical and perceptual characteristics have indicated that there are fundamental processing differences between first- and second-order motion perceptions. Three leading hypotheses describe the possible neural basis of first- and second-order motion perception. First, the two types of motion may be processed by separate neural substrates located in distinct cortical areas. The amount of neural separation between these two processes has varied from model to model, from pre-processing stage differences, to separate cortical representations. Secondly, the two types of motion may be processed in the same (or similar) channels located within the same cortical areas. Thirdly, form-driven or attentional tracking of moving features may support second-order motion more than luminance-based motion. Focused attention following moving features may be required to process second-order, but not first-order motion [23].

2.6 Computational Models of Motion Perception

The first computational account of motion perception arose five decades ago, from the collaboration of Bernhard Hassenstein, a physicist, and Werner Reichardt, a biologist (Borst, 2000). Their product was a simple multiplicative correlation detector made up of two, oppositely-tuned subunits. To understand the detector's operation, imagine that a spot light moves across the retina, successively stimulating different groups of adjacent photoreceptors one after another. To simplify, assume that the moving spot's direction caused the spot to fall first on photoreceptor A, and then, after some delay, Δt, on photoreceptor B. As a result, the luminance signal elicited from A precedes the signal generated from B by Δt. This delay depends upon two variables, the spatial separation between A and B, and the speed with which the spot moves. For one of the detector's subunits the luminance signal generated in photoreceptor A is multiplied by a delayed luminance signal from a second, neighboring photoreceptor set, B. This basic operation is replicated in the detector's other subunit, but in mirror-symmetrical fashion: the two photoreceptors are flip-flopped, and the delay is now applied to the signal from the

previously non-delayed photoreceptor. Because of the delays, a spot reaching first A and then B, generates a larger response in the second subunit than in the first; the same spot travelling at the same speed, but in the opposite direction generates a larger response in the first subunit than in the second. In other words, the numerical difference between the two subunits' responses is directionally selective: motion in one direction generates a positive difference, motion in the opposite direction a negative difference [10]. A version of the Reichardt model is shown in Figure 2.4.

The model's simple circuit guarantees that motion sensitivity will reflect a stimulus' temporal and spatial parameters, which is certainly true of vision. In its first tests, the model was applied to insect vision, exploiting as a behavioral index of motion perception in the optomotor reflex of the beetle Chlorophanus. The model's success inspired a good deal of research, including work on higher animals. It also promoted the creation of other models that performed a similar computation using different circuitry [10].

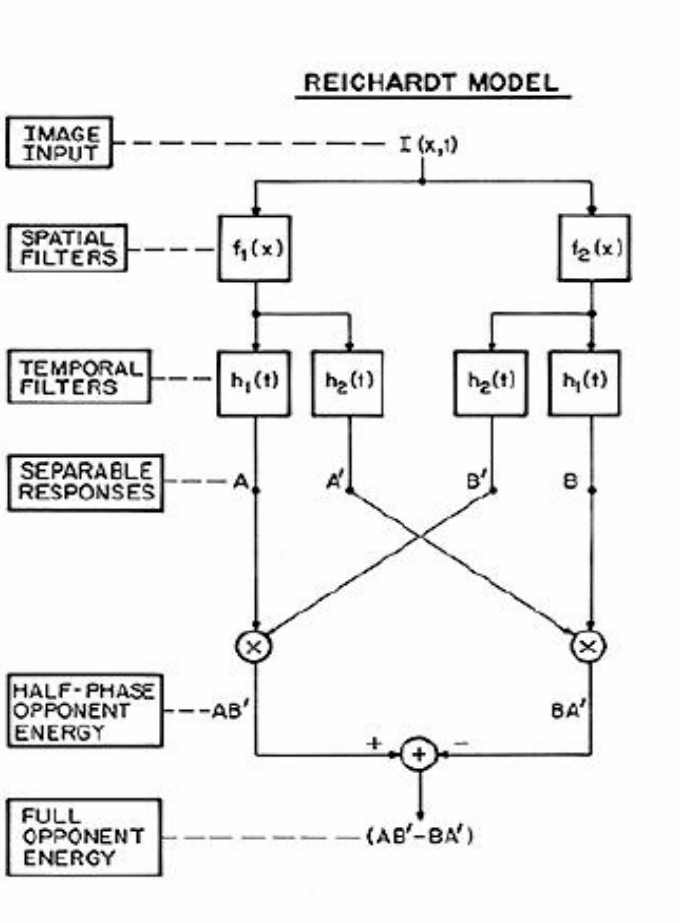

Figure 2.4 A version of the Reichardt model that is formally equivalent to a version of an energy model. The visual input I(x, t) passes through the two spatial impulse responses f1(x) and f2(x). Following van Santen and Sperling, these functions can be bandpass, differing in phase or in position. Each output passes through the two temporal functions h1(t) and h2(t) where h2(t) is more low passed or more delayed than h1(t). The four separable responses are labeled A, A', B, and B'. The products AB' and BA' are generated, and their difference constitutes the final output. (Adelson, Bergen, *Spatiotemporal Energy Models for the Perception of Motion*) [9].

Although the Hassenstein-Reichardt motion circuit has many virtues, it also has one property that could be considered a flaw: it fails to distinguish between two classes of stimuli that physically are quite different from one another. In particular, the circuit would give equivalent responses to a spot that moved smoothly with the proper velocity from the receptive fields of one subunit's receptors to the receptive fields of the other subunit's receptors, and a spot that was presented to one set of receptive fields, then extinguished, and after a delay, presented to the other receptive fields. With proper delays between presentations of the spot, this latter, sampled or stroboscopic motion stimulus, would be

indistinguishable from its smooth counterpart. Scaled up to an entire human visual system, this perceptual error becomes quite important. It allows the sampled images that comprise film and video sequences to mimic smooth motion. The result of such a sampling process is known as apparent motion, a designation meant to contrast with smooth or real motion. Much of the motion we view daily at the cinema and on television is not real motion but an illusion created by displaying a series of still pictures in rapid succession (24 Hz for cinema, 60 Hz for NSTC television). This type of motion is referred to as apparent motion, stroboscopic motion, or, most accurately, sampled motion. For some time it was thought that apparent motion may be detected by different processes from those detecting real motion, but recent studies find little justification for this view. Most motion detectors that incorporate spatiotemporal filtering will respond well to sampled motion, provided the sampling rate is sufficiently high. The spatiotemporal trajectory for apparent motion is a row of dots in space-time. If the spatiotemporal receptive fields are oriented parallel to this trajectory, they will integrate the discrete samples, effectively causing the motion to become continuous (Burr and Ross, 1986). The minimum theoretical sampling rate is given by the Nyquist limit, which requires that the image be sampled at least twice the temporal frequency of image motion. Sampling below this frequency will cause aliasing, well-illustrated by the so-called wagon-wheel effect: periodic moving stimuli, are seen to stop and reverse direction as the wagon accelerates. The quality of apparent motion varies with a number of parameters, particularly the rate at which the stimulus is sampled in both space and time domains. As the interval lengthens between successive frames of display, the sampling rate is said to decrease. Intuitively, as sampling rate increases and successive frames come closer together in time, the appearance of the sampled stimulus approaches that of a smoothly-moving stimulus. When the repetition frequency of spokes exceeds half the sampling frequency (12 Hz for cinema), it will be undersampled, creating strong aliasing in the form of erroneous motion. The conditions under which sampled motion is indistinguishable from smooth motion can be predicted quantitatively from measurements of contrast sensitivity and linear systems analysis (Burr, Ross, and Morrone, 1986). Sampling a motion signal introduces spurious artifacts, whose frequency and amplitude depend on the sampling rate. Psychophysical measurements show that subjects are able to distinguish sampled from smooth motion if and only if the spurious frequencies produced by the sampling regime are not resolvable, as determined by measuring their thresholds for

isolated sinusoids. The spatiotemporally oriented receptive fields not only allow for the perception of discontinuous motion, but can also cause the image to be interpolated between the positions where it is displayed on each sample. The extrapolation is extremely accurate, and works over long ranges. Indeed, this property can be used to generate complex spatial forms from temporal information alone (Burr and Ross, 1986). When moving forms pass behind a "virtual slatted fence" (allowing information to be displayed only at discrete points), the visual system interpolates between the display points to give the impression of complete spatial forms. Thus, motion detectors not only encode velocity information about moving objects, but also participate in their spatial analysis [10].

Watson, Ahumada and Farrell developed a simple model that predicts whether any spatial and temporal sampling rate would or would not produce the appearance of smooth motion [11]. Their model defines a spatiotemporal range of each observer's window of visibility. The boundaries of this window, a region in joint spatial and temporal frequency space, define the spatial and temporal frequency limits of the observer's sensitivity to energy in the stimulus. When the stimulus is sampled in time, as for video or film or computer displays, the sampling process generates energy at temporal frequencies in addition to the fundamental frequency. A low sampling rate produces energy over a range of low temporal frequencies; a high sampling rate produces energy over a range of high temporal frequencies. As a result, the higher the sampling rate, the more likely it is that the resulting energy will fall outside the window of visibility, which renders them invisible and perceptually inconsequential. So two stimuli, one smoothly moving and the other representing sampled motion, will appear identical if their spectra within the window of visibility are identical; portions of their spectra that lie outside the window are irrelevant. Using two different strategies for sampling stimuli, Watson and colleagues confirmed the essential validity of their elegantly simple model [11].

Following Hassenstein and Reichardt, most studies of motion perception have examined responses to drifting modulations of luminance or chromatic contrast. These stimuli, termed first-order stimuli or Fourier stimuli, would evoke responses in visual mechanisms responsive to spatiotemporal variation in luminance or chromatic contrast. Such stimuli correspond to a dominant species of spatiotemporal modulation encountered

everyday, but such stimuli do not exhaust the possibilities. Some stimuli, termed second-order or non-Fourier stimuli, would elude detection by such mechanisms [10]. Second-order stimuli, such as the motion of a contrast modulation over a texture, have the property of being characterized in the spatiotemporal Fourier domain by power spectra which are displaced away from the frequency space origin. Observers can readily perceive second-order motion and it has been postulated that there exists separate channels specifically to process second order signals. These second-order detecting mechanisms rely on a pre-processing step which carries out an explicit rectification of the stimulus to recover a luminance signal that can then be processed with standard Fourier energy methods [12].

Figure 2.5 and 2.6 show examples of first- and second-order patterns. In Figure 2.5, a sinusoidal luminance grating has been added to a random noise pattern to make the first-order pattern whereas in Figure 2.6, the contrast of the random noise has been modulated sinusoidally over space to make the second-order pattern. The orientation of the contrast-modulation cannot be detected by linear (first-order) mechanisms as the expected luminance of any region of the image is the same, so some form of non-linear (second-order) mechanism is required [13].

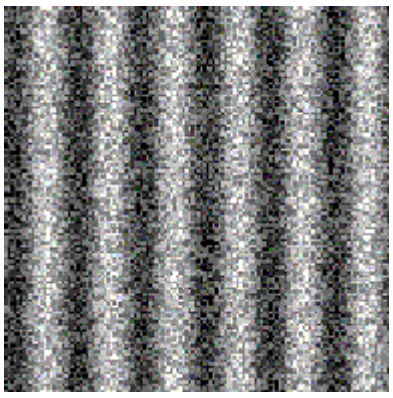

Figure 2.5 First-order pattern [13].

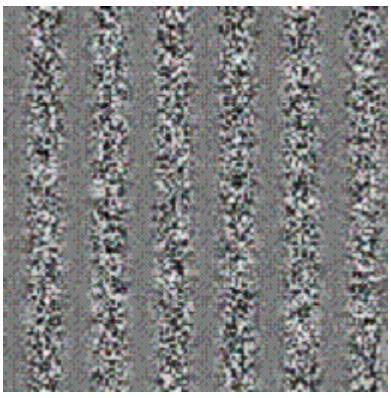

Figure 2.6 Second-order pattern [13].

3. MATERIALS AND METHODS

3.1 Subjects

Ten subjects (five males and five females, age: 18-25) with normal visual acuity were tested. They were naive about the purpose of the experiment. All subjects provided written consent for their participation. Each subject spent approximately 2 hours in 4 sessions to complete the experiment.

3.2 Apparatus

The visual stimuli were presented on a calibrated CRT monitor (Samsung SyncMaster 551v). The subjects viewed stimuli from a distance of 50 cm and subtended an angle of 2.39º from the center. Testing was performed binocularly. The head movements were minimized using a chin-rest and forehead-rest (Figure 3.1).

Figure 3.1 The picture of the experimental setup.

Before the experiments, the stimuli were calibrated. The luminances of the gray levels are shown in the Figure 3.2.

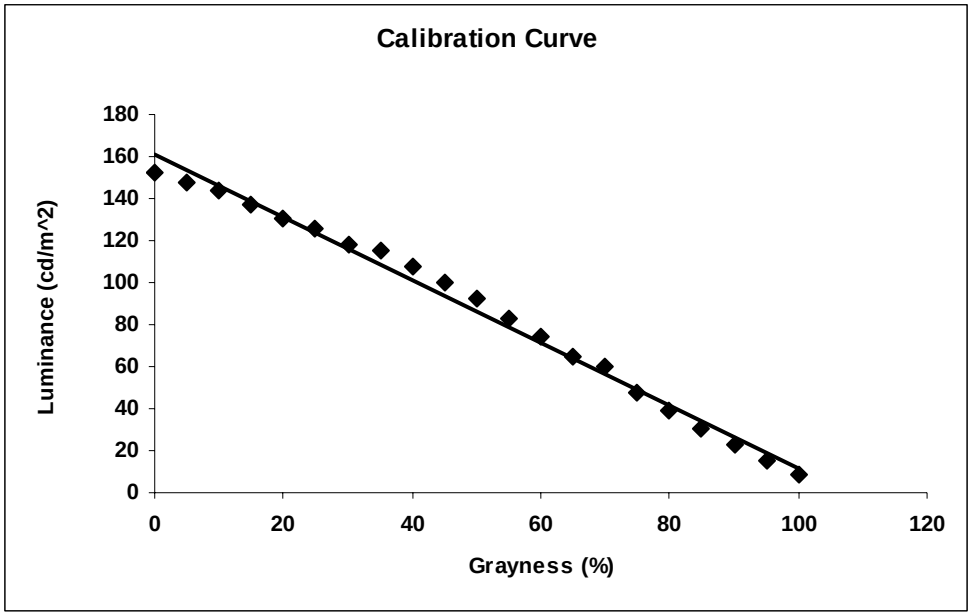

Figure 3.2 Calibration plot.

3.3 Stimuli

The stimuli were generated on a PC and presented using a MATLAB program (see Appendix A.1.1).

The stimuli were created using CorelDRAW and Adobe Photoshop. The stimuli were filled squares presented on a Gaussian noise pattern with a 50% gray level (95.66 cd/m^2) mean luminance background (Figure 3.3). The dimensions of the filled squares were 3x3 cm.

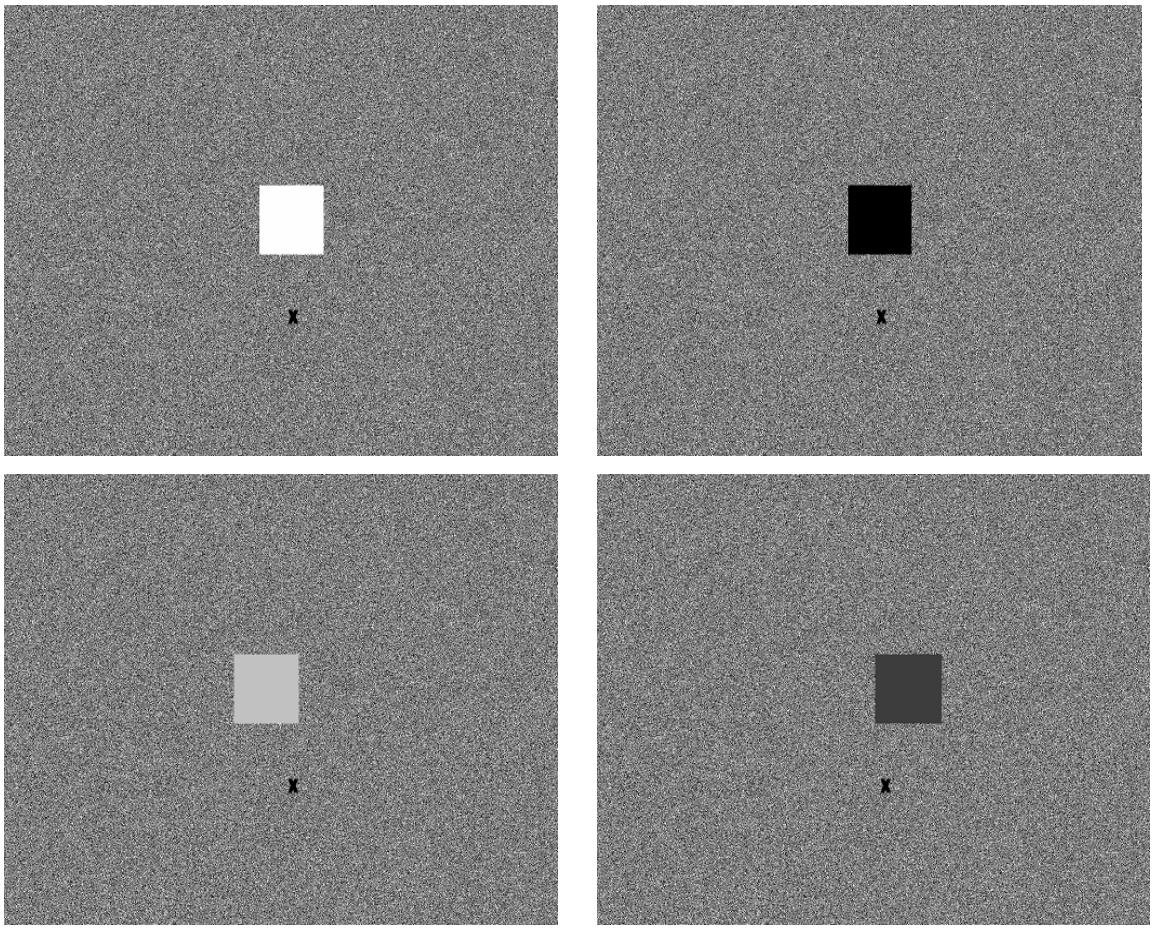

Figure 3.3 Stimulus examples.

There were 24 stimulus conditions (movies) as shown in Table 3.1. The motion direction was towards left for the 12 movies and towards right for the other 12 movies. Initial and terminal luminance values were randomly selected to be 100%, 65%, 35%, 0% grayness corresponding to 9, 65, 115, 153 cd/m^2. For each stimulus condition, two sets of initial and terminal luminance values were selected. There are 6 movies for each initial and terminal luminance values. The stimuli are randomly presented in a factorial design.

There are 3 factors:

Factor 1: The luminance of the target at the motion instant (75%, 50%, 25% grayness corresponding to 47, 92, 125 cd/m^2)

Factor 2: The direction of the motion; right or left

Factor 3: The luminance-change direction; bright to dim or dim to bright

The luminance-change was incremented or decremented by 5% grayness. Speed of the stimulus was constant for each movie and it was 0.16º/s. Inter-stimulus interval was selected to be 0.128s. Luminance sweep rate was 56.13 cd/m²/s.

Below the stimulus, a fixation cross was presented. The distance between stimulus and fixation cross was 2.5 cm.

Table 3.1

24 movies as stimulus conditions. Initial grayness (%), terminal grayness (%), direction and grayness at motion instant (%) are shown in columns.

Stimulus	Initial Grayness (%)	Terminal Grayness (%)	Direction	Grayness at Motion Instant (%)
avi_1	0	35	Right	25
avi_2	0	35	Left	25
avi_3	0	65	Right	25
avi_4	0	65	Left	25
avi_5	0	100	Right	75
avi_6	0	100	Left	75
avi_7	35	0	Right	25
avi_8	35	0	Left	25
avi_9	35	65	Right	50
avi_10	35	65	Left	50
avi_11	35	100	Right	50
avi_12	35	100	Left	50
avi_13	65	0	Right	25
avi_14	65	0	Left	25
avi_15	65	35	Right	50
avi_16	65	35	Left	50
avi_17	65	100	Right	75
avi_18	65	100	Left	75
avi_19	100	0	Right	75
avi_20	100	0	Left	75
avi_21	100	35	Right	50
avi_22	100	35	Left	50
avi_23	100	65	Right	75
avi_24	100	65	Left	75

3.4 Procedure

The experimental procedure was matching to the grayness value on the gray scale. The experiments were completed in 4 sessions. Randomly selected 24 movies were shown in each session. Four measurements were taken from each subject for a given stimulus condition. Each subject was initially trained how to view images. Movies were played alternately and continuously when the program had been executed. Each stimulus was presented 10 times. Subjects were instructed to press a mouse button when they were sure about the matched grayness value. Otherwise the same stimulus was presented again. Four measurements were taken from the subjects in order to get the mean value of the responses.

Initially, the square was in the middle of the screen. Images transformed from bright to dim or dim to bright and at a certain grayness value (25%, 50%, 75% grayness), the square moved towards left or right. After each movie was shown, a list of standard grayscale images (5% gray level increments) appeared for matching to the luminance at motion instant (Figure 3.4). What was asked from the subjects was to fixate their eyes to the fixation cross and match the luminance value on the gray scale when the motion occured, either towards left or right. The task also required to keep luminance information in memory. This matching procedure was shown by hand.

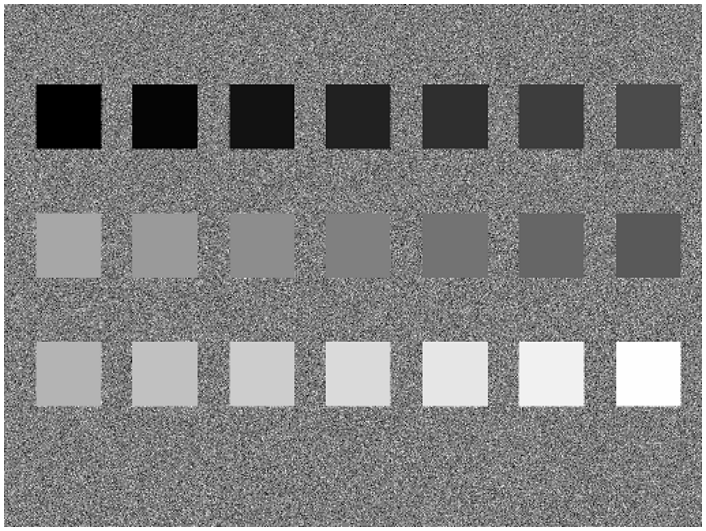

Figure 3.4 A list of standard grayscale images for matching to the luminance at motion.

3.5 Analyses

The difference between the presentation time of matched values gave the time-lag, i.e. asynchronism, between luminance and motion perception.

ANOVA was performed in MATLAB to determine interactions between factors and to study main effects.

3.6 Computational Model

A computational model was used to predict the results of the current experiment. Figure 3.5 shows the block diagram of the model. The model was inspired by Elaborated Reichardt Model of vision and further modified in MATLAB [9]. The model included two inputs from adjacent retinal locations and two outputs. One output was from the luminance processing channel, and the other output was from the motion processing channel. The motion processing channel is based on the multiplication of two signals that are time-lagged with each other. Because of the delays, signals reaching to the different locations generate different responses. There is a larger response in the second subunit than in the first. But in the opposite direction, a larger response is generated in the first subunit than in the second. The numerical difference between the subunits indicates that the motion in one way will make a positive difference and the motion in the opposite direction will make negative difference. In other words, the outputs of the two multiplications are subtracted to give a single time-dependent correlator output.

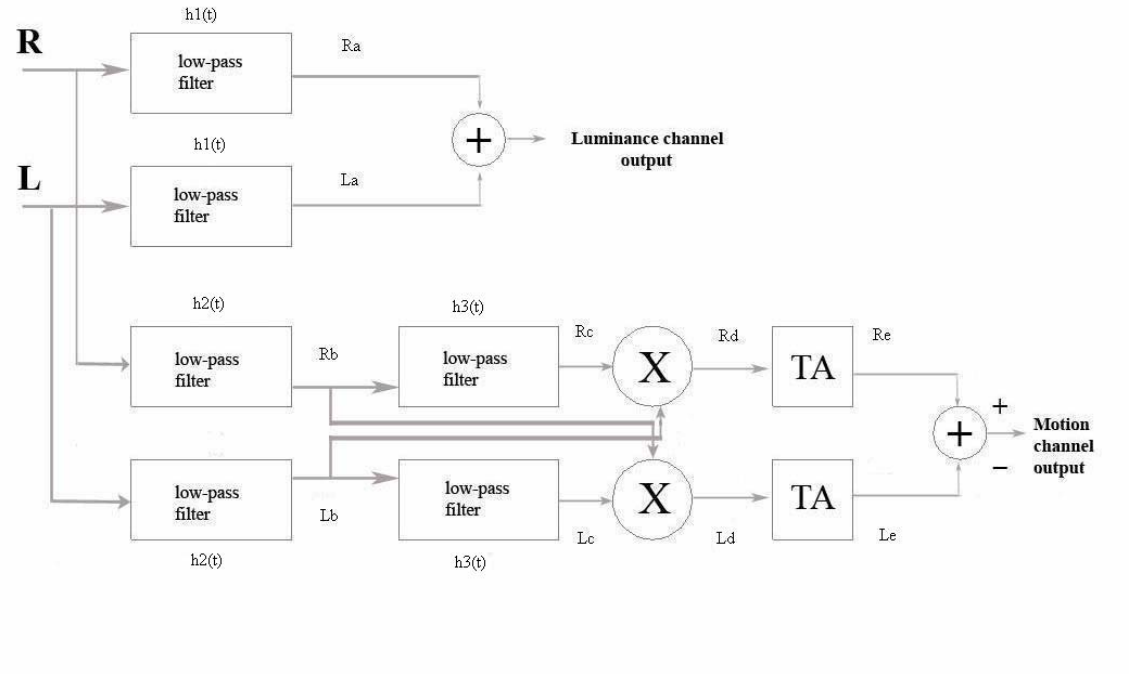

Figure 3.5 Block diagram of the computational model.

The luminance channel had temporal filters at the input side and summated the processed inputs to produce an output. As shown in Figure 3.5, the input filters were approximated as first-order low-pass filters with impulse responses as

$$h_1(t) = (1/\tau).\exp(-t/\tau_1) \qquad (3.1)$$

$$\tau_1 = 1.3 \text{ s}$$

The time constant for the luminance channel was determined according to Kerzel's experiment [2]. The range between 1 s and 1.5 s was tested. 1.3 s was selected experimentally to get the appropriate and explicit simulated neural activity curve.

$R_a(t)$ and $L_a(t)$ are the outputs of temporally low-pass filtered retinal inputs, R(t) and L(t).

In order to calculate $R_a(t)$ and $L_a(t)$, Equations 3.3 and 3.4 were used.

$$R_a(t) = R(t) * h_1(t) \quad (3.2)$$

$$L_a(t) = L(t) * h_1(t) \quad (3.3)$$

Numerous electrophsiological and behavioral studies have refined and elaborated the Reichardt Model. The retinal signal, as sampled by the photoreceptors, has already been blurred spatially due to diffraction effects of the lens optics as well as the properties of the photoreceptors themselves (Snyder, 1979). The photoreceptors can not respond with infinite speed to changes in illumination, so they act as low-pass temporal filters.

Therefore, the motion channel had also temporal low-pass filters at the input side. The impulse response of the input filters are:

$$h_2(t) = (1/\tau).\exp(-t/\tau_2) \quad (3.4)$$

$\tau_2 = 0.008$ s

In order to calculate $R_b(t)$ and $L_b(t)$, the following equations were used.

$$R_b(t) = R(t) * h_2(t) \quad (3.5)$$

$$L_b(t) = L(t) * h_2(t) \quad (3.6)$$

The next low-pass filter is the delay filter of the motion channel and has the time constant $\tau_3 = 0.035$ s.

$$h_3(t) = (1/\tau).\exp(-t/\tau_3) \quad (3.7)$$

Choosing of time constants is based on the motion-plus-pedestal paradigm (Lu & Sperling, 1996).

$$R_c(t)=R_b(t)*h_3(t) \quad (3.8)$$

$$L_c(t)=L_b(t)*h_3(t) \quad (3.9)$$

The model agreed fairly well with physiological data and it facilitated analysis as well as estimation of the constants involved. As van Santen and Sperling (1985) pointed out, the performance of a correlator composed of two subunits does not depend critically on the exact form of the delay filter. The delay filter determines the temporal frequency tuning, and therefore the response to different motion velocities.

The next operation is multiplication (X) of the left and the right subunits (Figure 3.5). Equations 3.13 and 3.14 were used to calculate the output values.

$$R_d(t) = L_b(t) \,.\, R_c(t) \quad (3.10)$$

$$L_d(t) = R_b(t) \,.\, L_c(t) \quad (3.11)$$

Most models of correlator-based motion detection have included some temporal integration in the motion channel. Such integration in space and time must occur at some point in a biological visual system to produce coherent reactions to visual stimuli. The early Reichardt models included infinite temporal averaging. This model included finite temporal averaging, represented as TA in Figure 3.5. It was integrated over a finite amount of time (Δt = 100 ms).

According to Figure 3.5,

$$R_e(t) = (1/\Delta t). \int_{t-\Delta t}^{t} R_d(t')dt' \quad (3.12)$$

$$L_e(t) = (1/\Delta t). \int_{t-\Delta t}^{t} L_d(t')dt' \quad (3.13)$$

Generally, the response function of sensory organs is logarithmic, which means that for a weak stimulus, a small change in stimulus strength is detectable, whereas for a strong

stimulus, the change must be larger to be detected (Weber's law: detectable stimulus strength difference proportional to stimulus strength). The computational model was linked to psychophysics by using difference limens in Weber's law. Luminance and motion discrimination thresholds are typically presented as Weber fractions (ΔL/L, ΔM/M) to produce reliable discrimination. The smallest increment in luminance that can be reliably detected (ΔL) is divided by the mean or base value (L). Similarly, the smallest increment in motion that can be reliably detected (ΔM) is divided by the mean or base value (M). A smaller Weber fraction reflects better discrimination performance.

For luminance channel, the Weber fraction was

$$\Delta L/L = 0.025 \quad [14]$$

and for motion channel, the Weber fraction was

$$\Delta M/M = 0.44 \quad [15]$$

Most studies have reported Weber fractions around these values, with various types of stimuli, including moving squares, dot fields, or sinusoidal gratings (Lu & Sperling, 1996; McKendrick & Badcock, & Morgan, 2004; Carreno & Zoido, 2001).

By using these Weber constants, psychophysical discrimination times were determined according to the channel outputs. The lag between the discrimination times was recorded as the asynchrony between the luminance and motion channels (see Appendix A.1.2, A.1.3).

4. RESULTS

4.1 Experimental Results

The graphics below show the responses of ten subjects according to a given factor. The blue points show the mean responses that the observers gave. The pink line shows the luminance value of % grayness at the motion instant. There are two graphics for each stimulus condition. One of them shows the mean responses of the left motion and the other one shows the mean responses of the right motion. The first five subjects are the male subjects and the last five subjects are the female subjects.

Figure 4.1 shows the mean responses of the subjects when the motion occurred towards left and Figure 4.2 shows the mean responses of the subjects when the motion occurred towards right. Both of them show that the subjects matched the luminance value after the motion that occured towards the luminance-change direction whether the direction was towards right or left.

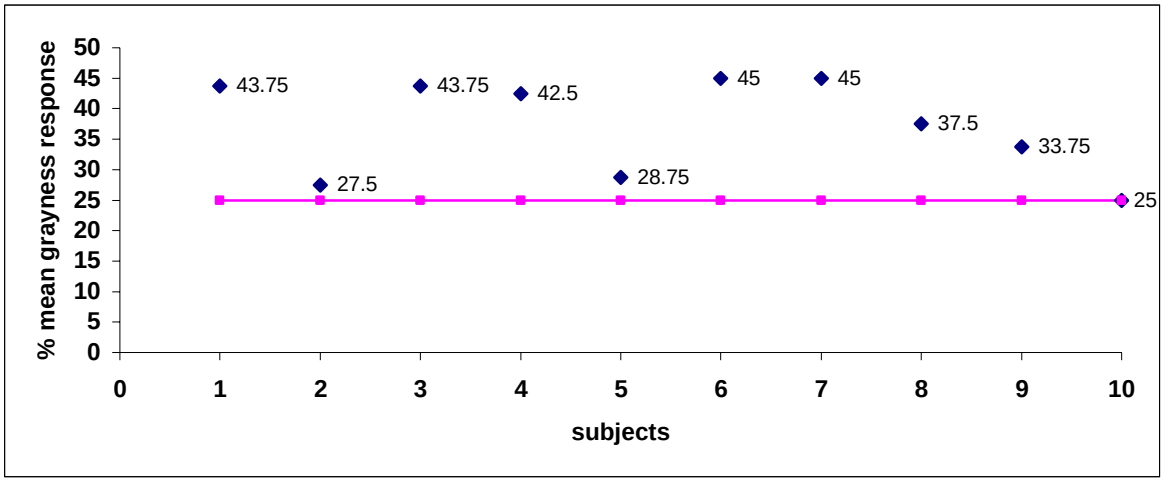

Figure 4.1 Matching results for 25% grayness at motion instant. Initial and terminal luminance values were 0% and 35%. Right motion.

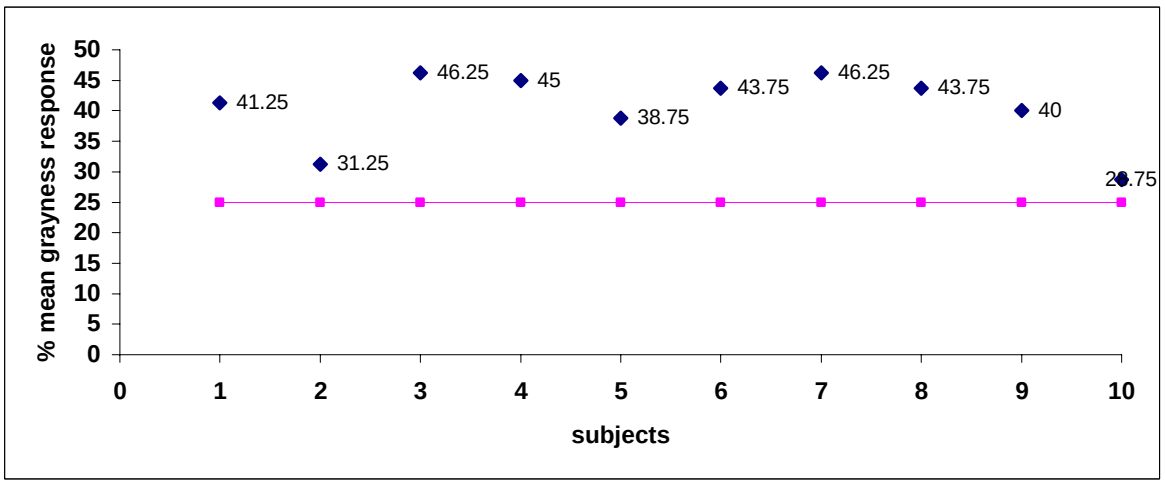

Figure 4.2 Matching results for 25% grayness at motion instant. Initial and terminal luminance values were 0% and 35%. Left motion.

Similarly, in the following figures, luminance-change direction made no difference or in other words, the motion direction had no effect on the match of the luminance value at the motion instant towards the luminance-change direction.

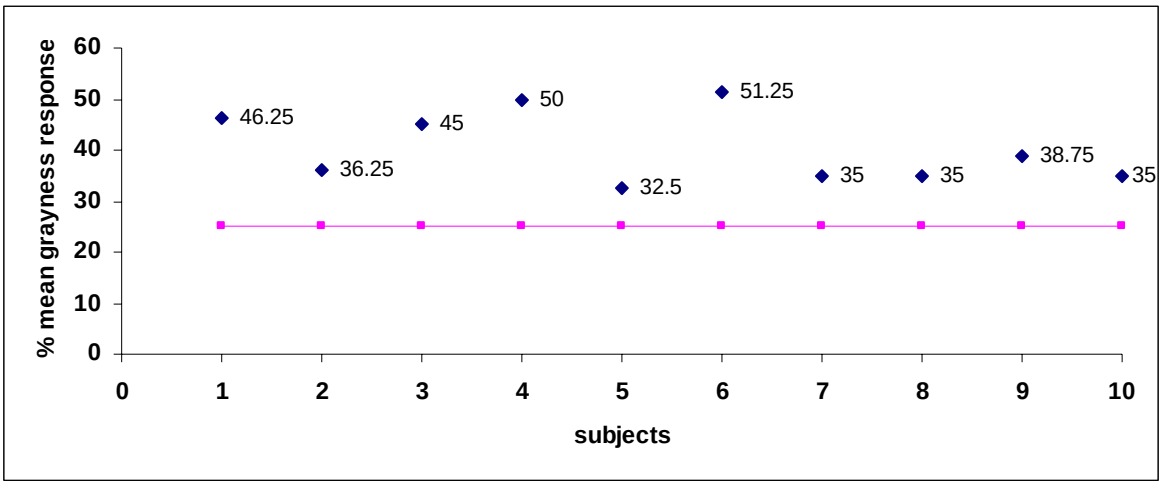

Figure 4.3 Matching results for 25% grayness at motion instant. Initial and terminal luminance values were 0% and 65%. Right motion.

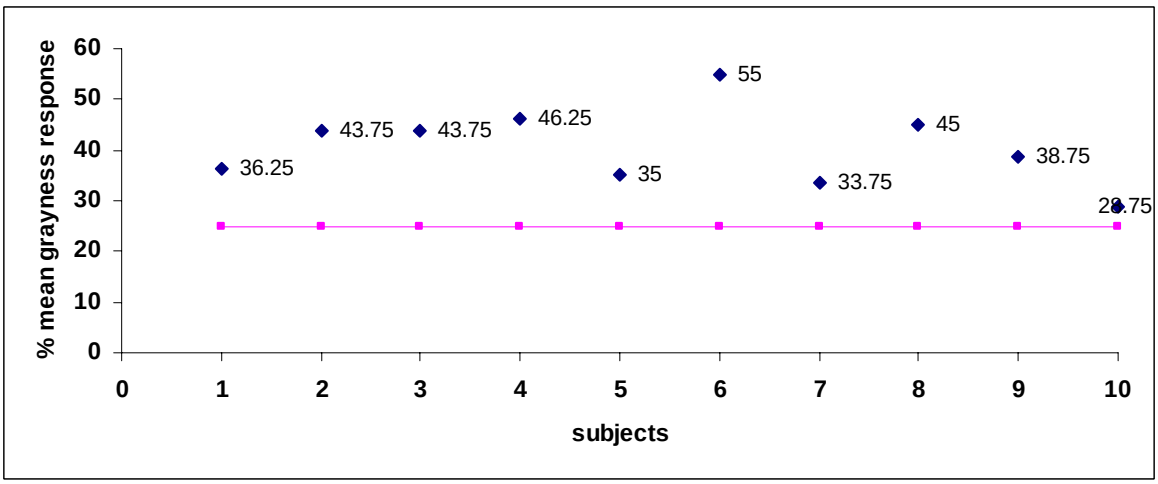

Figure 4.4 Matching results for 25% grayness at motion instant. Initial and terminal luminance values were 0% and 65%. Left motion.

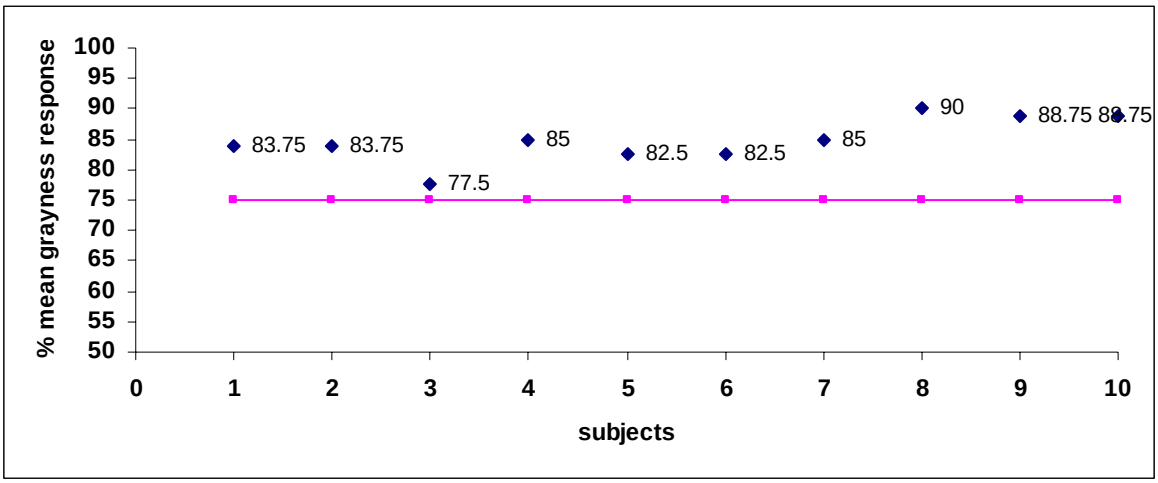

Figure 4.5 Matching results for 75% grayness at motion instant. Initial and terminal luminance values were 0% and 100%. Right motion.

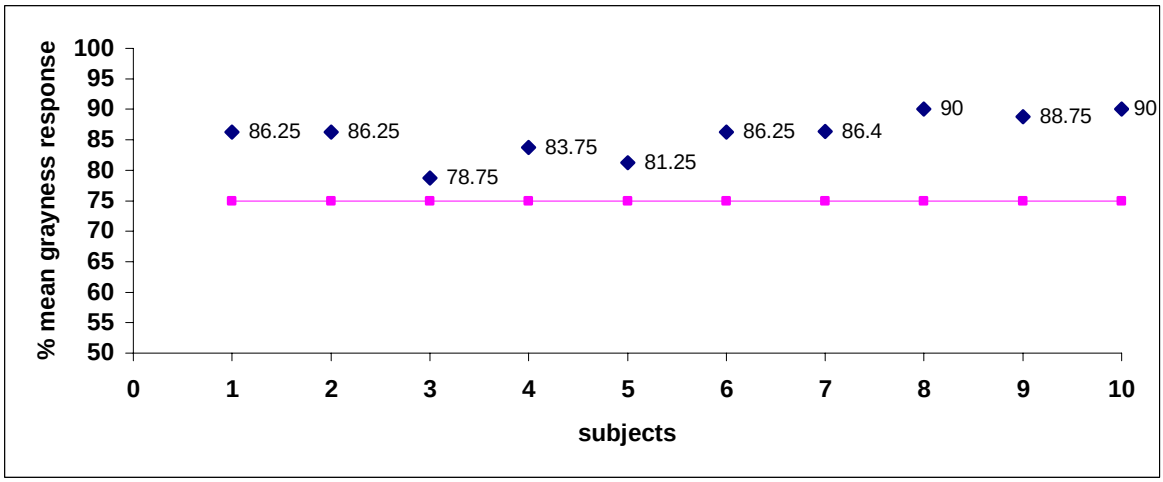

Figure 4.6 Matching results for 75% grayness at motion instant. Initial and terminal luminance values were 0% and 100%. Left motion.

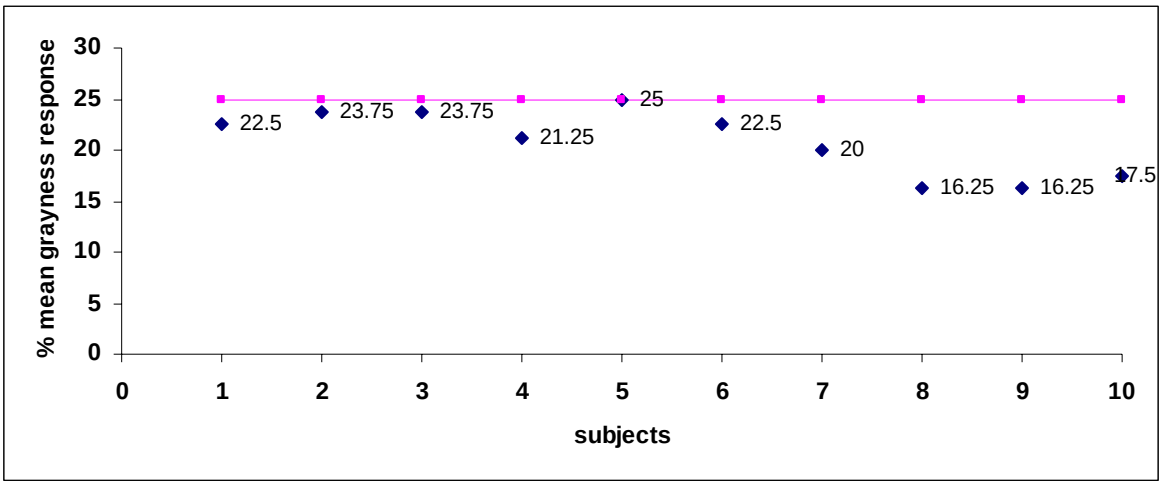

Figure 4.7 Matching results for 25% grayness at motion instant. Initial and terminal luminance values were 35% and 0%. Right motion.

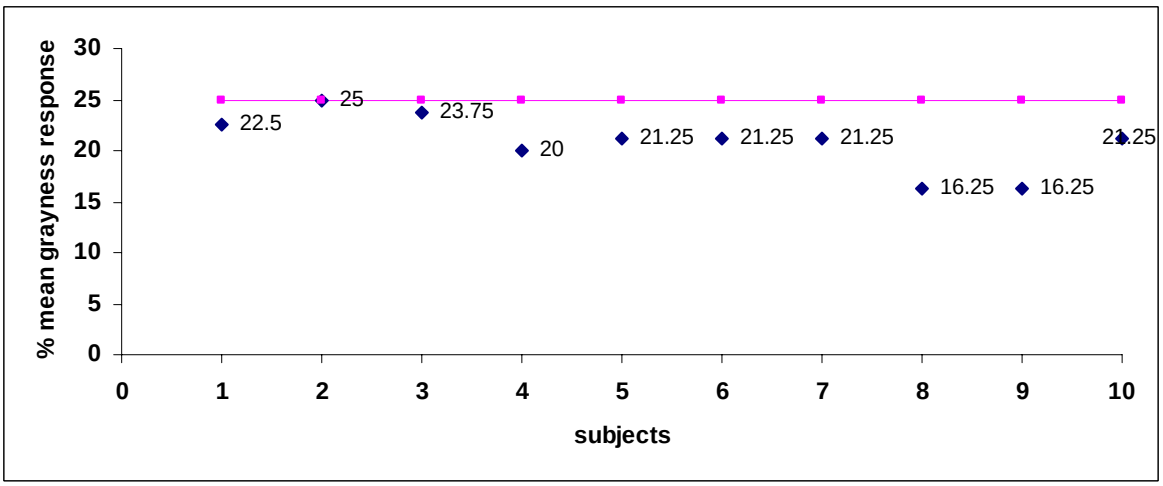

Figure 4.8 Matching results for 25% grayness at motion instant. Initial and terminal luminance values were 35% and 0%. Left motion.

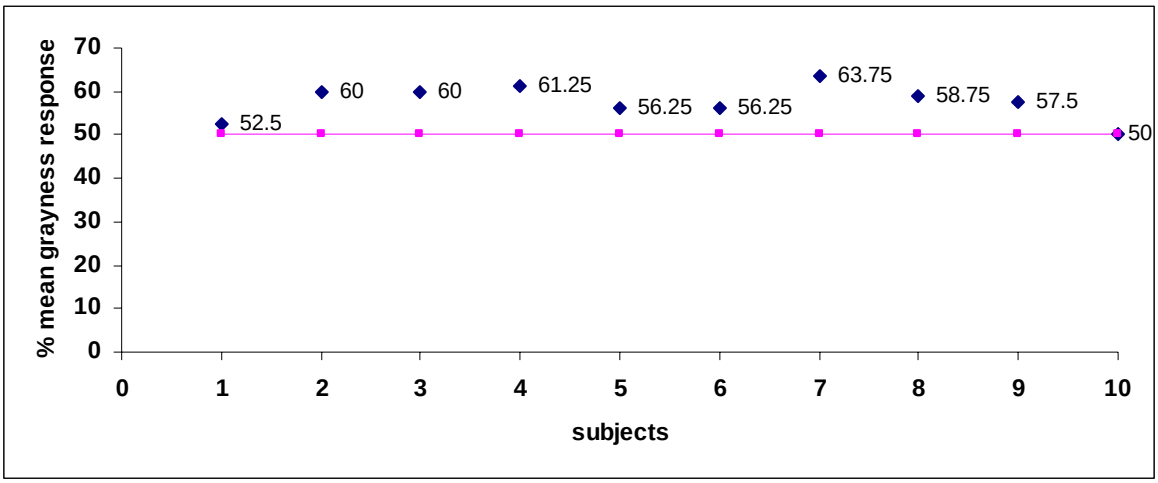

Figure 4.9 Matching results for 50% grayness at motion instant. Initial and terminal luminance values were 35% and 65%. Right motion.

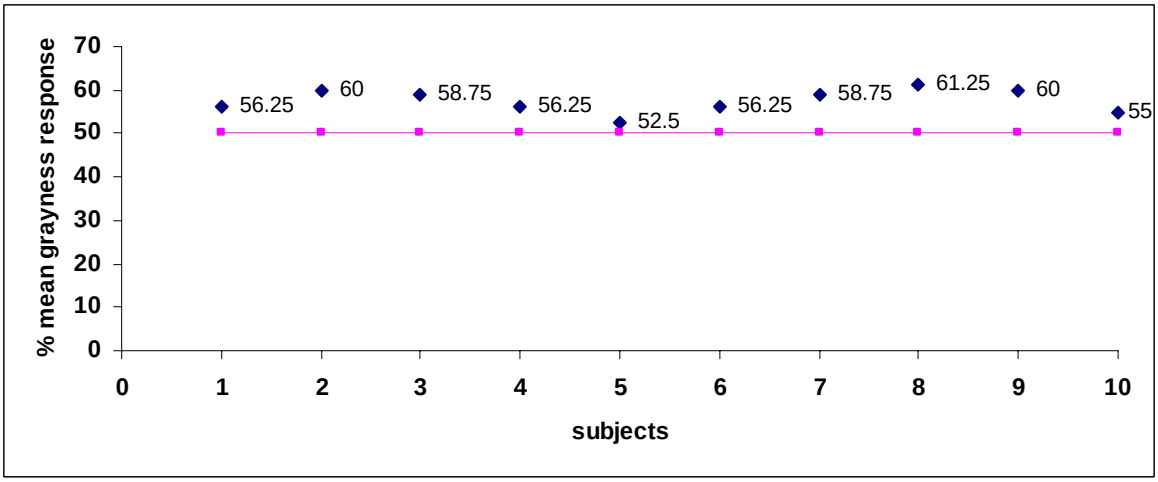

Figure 4.10 Matching results for 50% grayness at motion instant. Initial and terminal luminance values were 35% and 65%. Left motion.

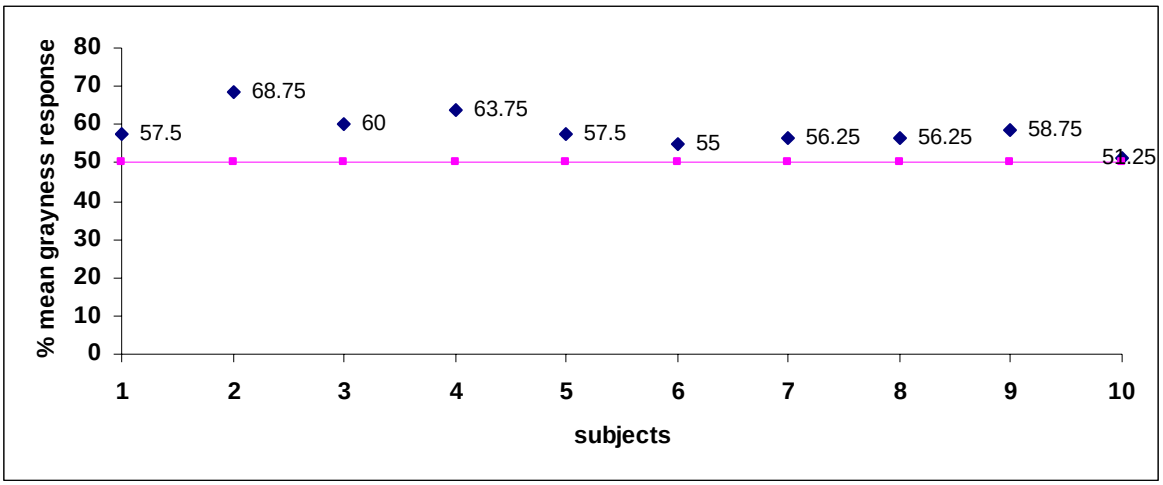

Figure 4.11 Matching results for 50% grayness at motion instant. Initial and terminal luminance values were 35% and 100%. Right motion.

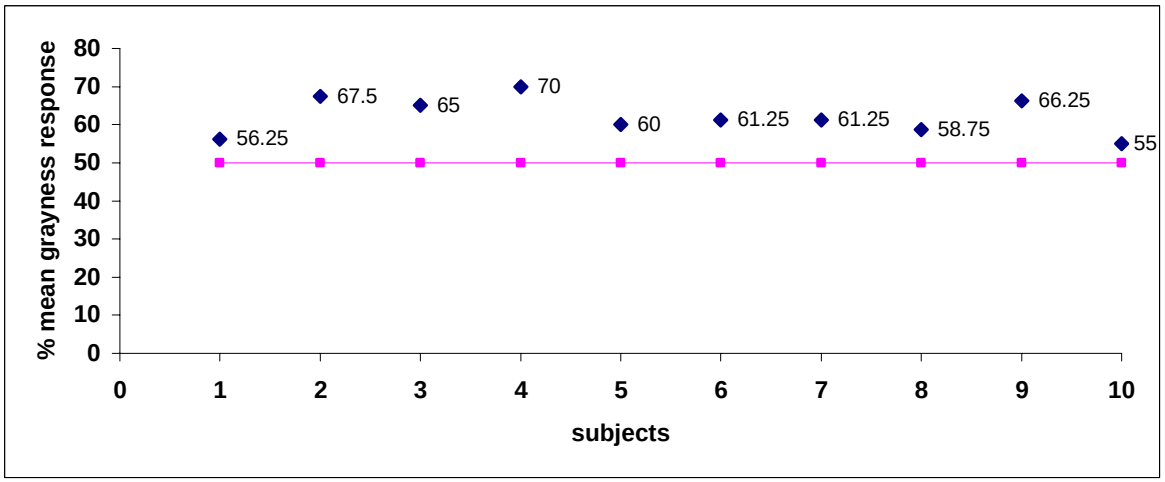

Figure 4.12 Matching results for 50% grayness at motion instant. Initial and terminal luminance values were 35% and 100%. Left motion.

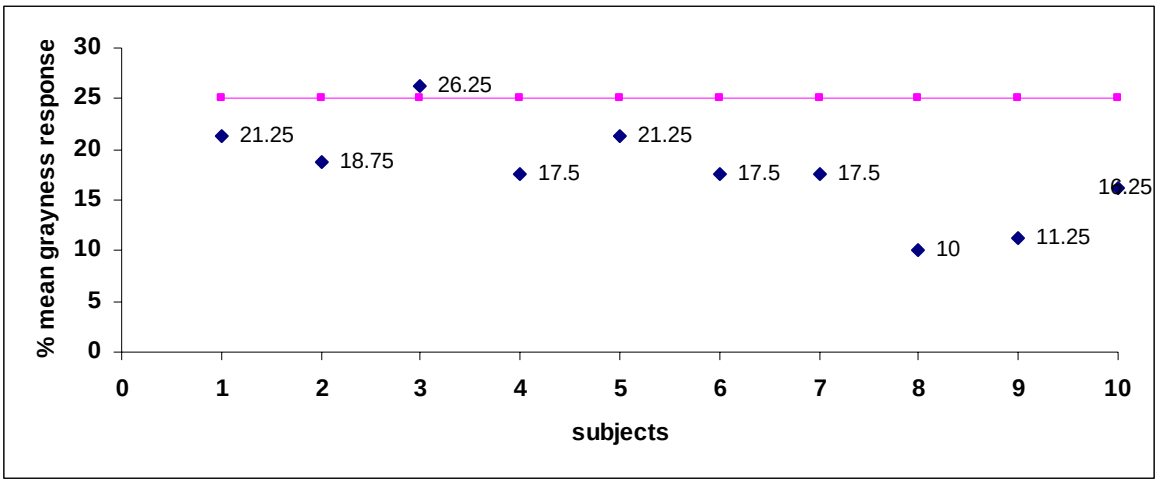

Figure 4.13 Matching results for 25% grayness at motion instant. Initial and terminal luminance values were 65% and 0%. Right motion.

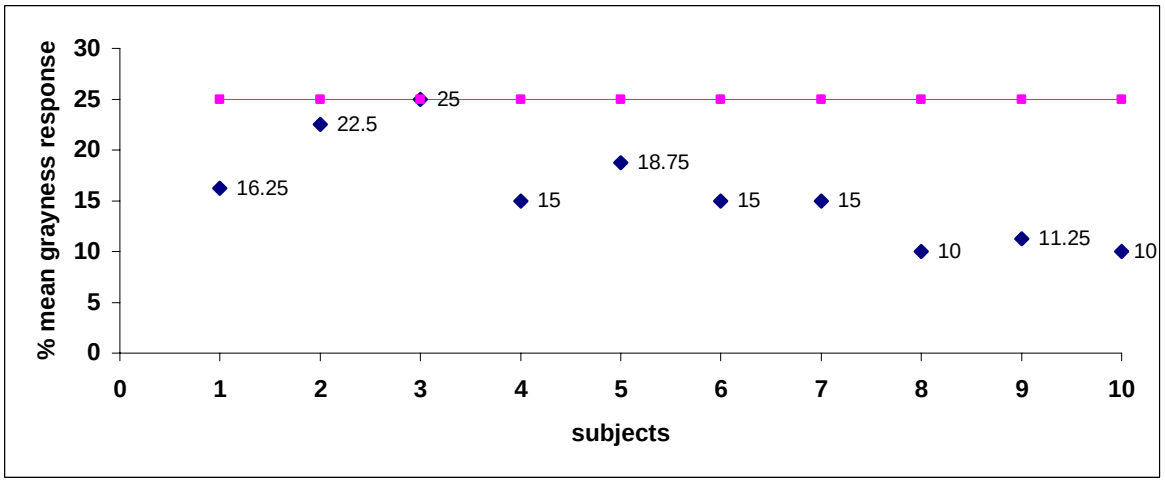

Figure 4.14 Matching results for 25% grayness at motion instant. Initial and terminal luminance values were 65% and 0%. Left motion.

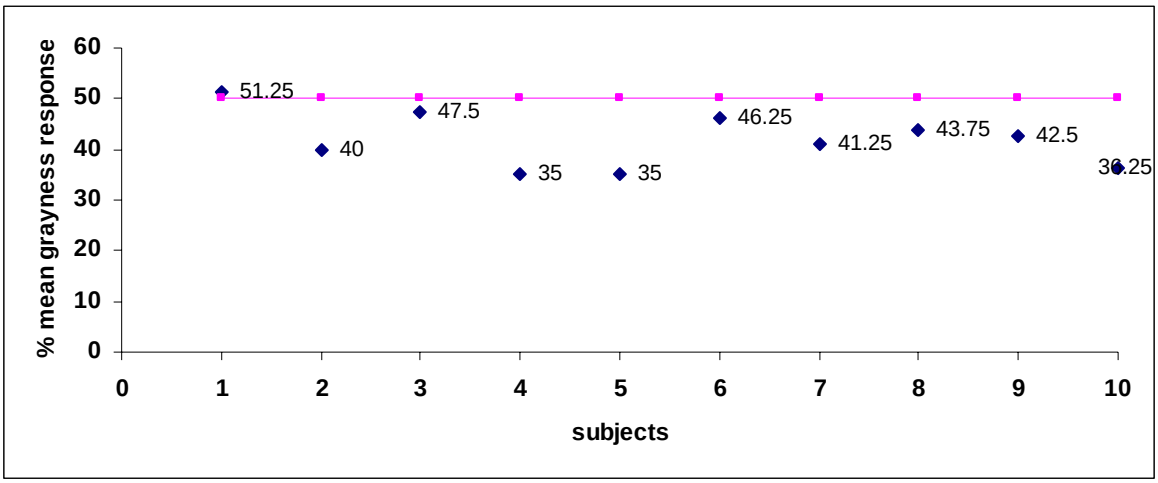

Figure 4.15 Matching results for 50% grayness at motion instant. Initial and terminal luminance values were 65% and 35%. Right motion.

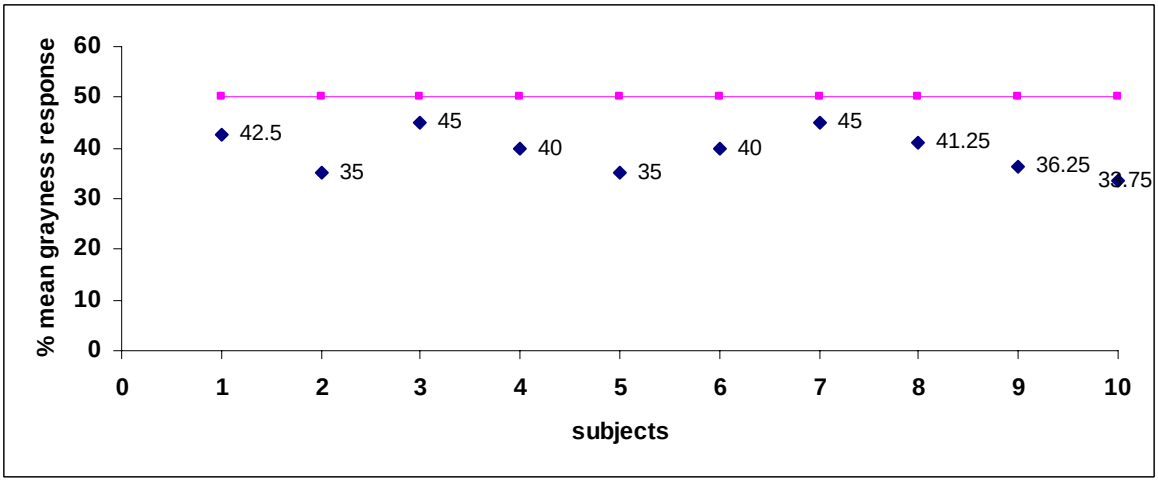

Figure 4.16 Matching results for 50% grayness at motion instant. Initial and terminal luminance values were 65% and 35%. Left motion.

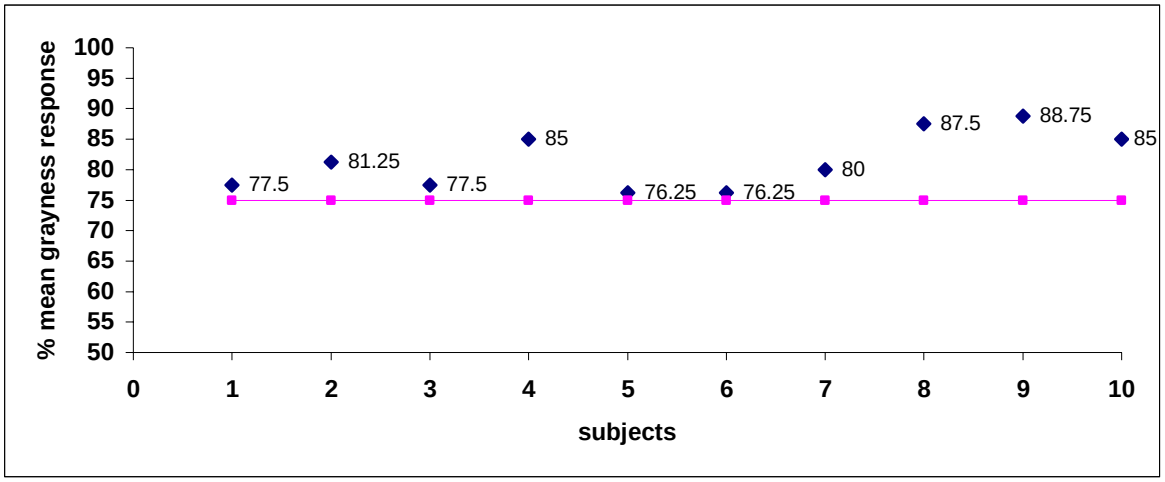

Figure 4.17 Matching results for 75% grayness at motion instant. Initial and terminal luminance values were 65% and 100%. Right motion.

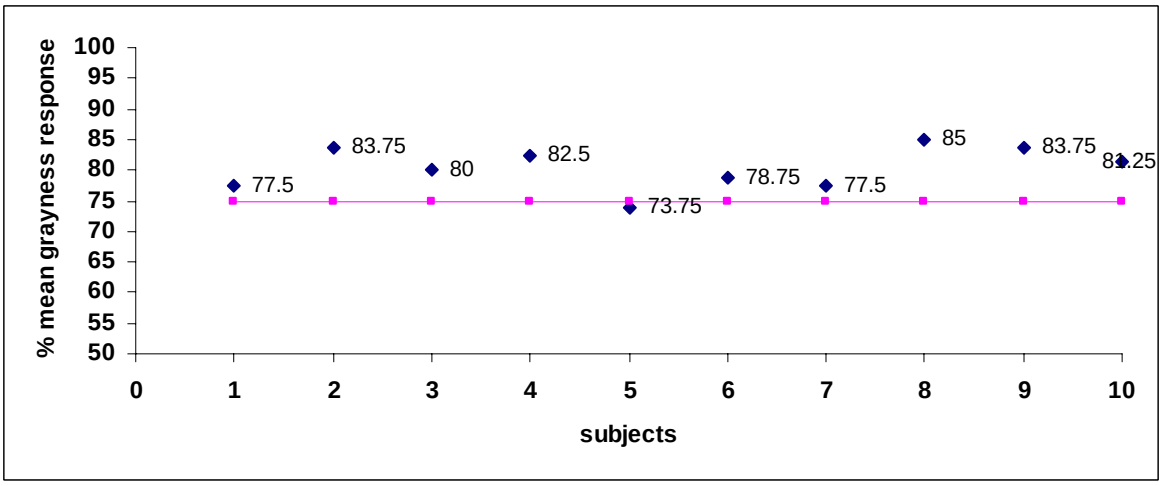

Figure 4.18 Matching results for 75% grayness at motion instant. Initial and terminal luminance values were 65% and 100%. Left motion.

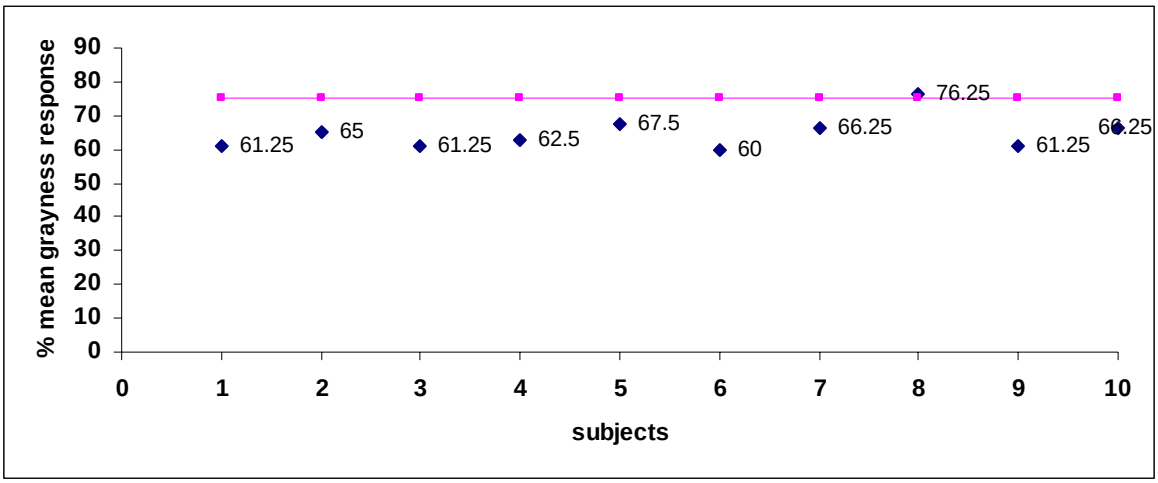

Figure 4.19 Matching results for 75% grayness at motion instant. Initial and terminal luminance values were 100% and 0%. Right motion.

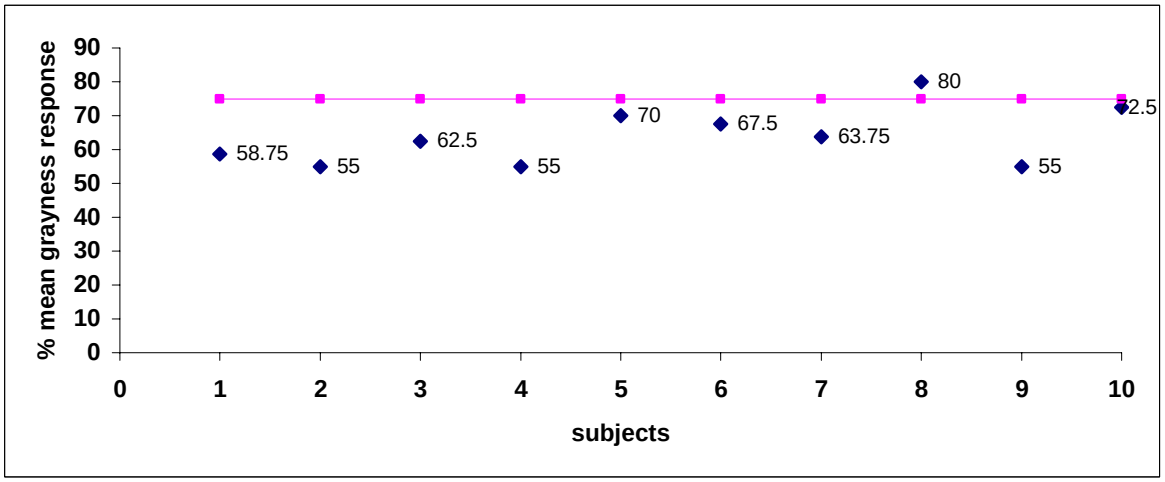

Figure 4.20 Matching results for 75% grayness at motion instant. Initial and terminal luminance values were 100% and 0%. Left motion.

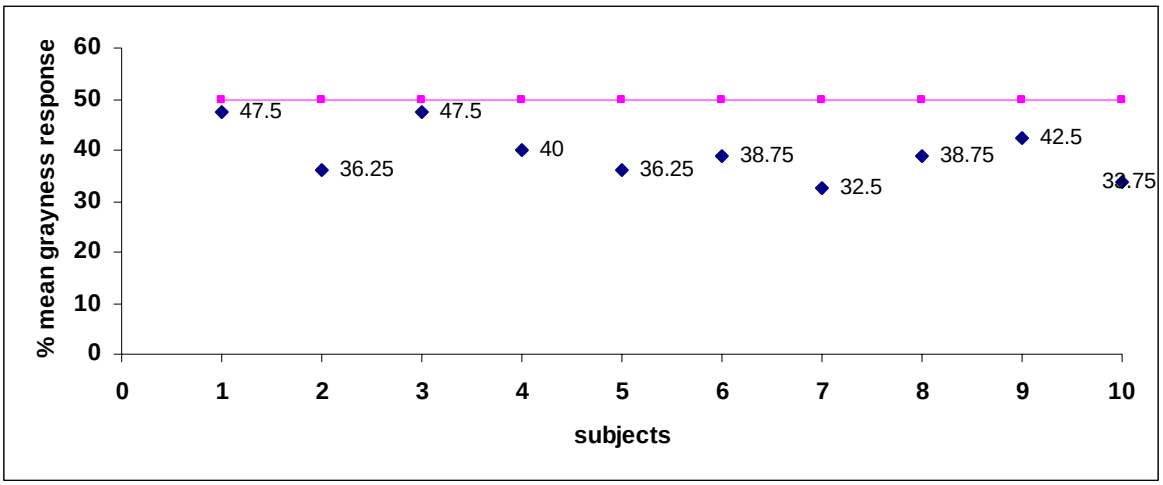

Figure 4.21 Matching results for 50% grayness at motion instant. Initial and terminal luminance values were 100% and 35%. Right motion.

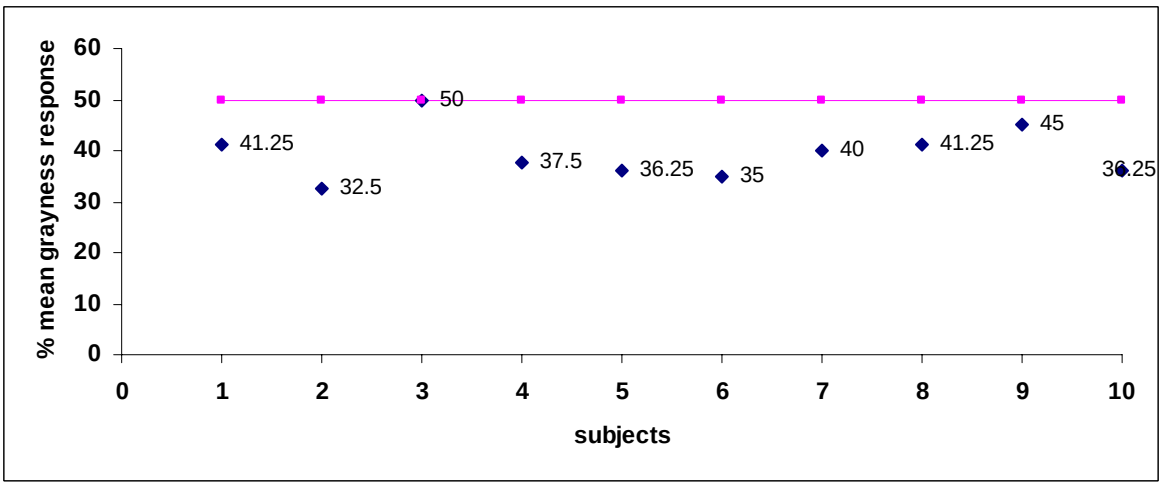

Figure 4.22 Matching results for 50% grayness at motion instant. Initial and terminal luminance values were 100% and 35%. Left motion.

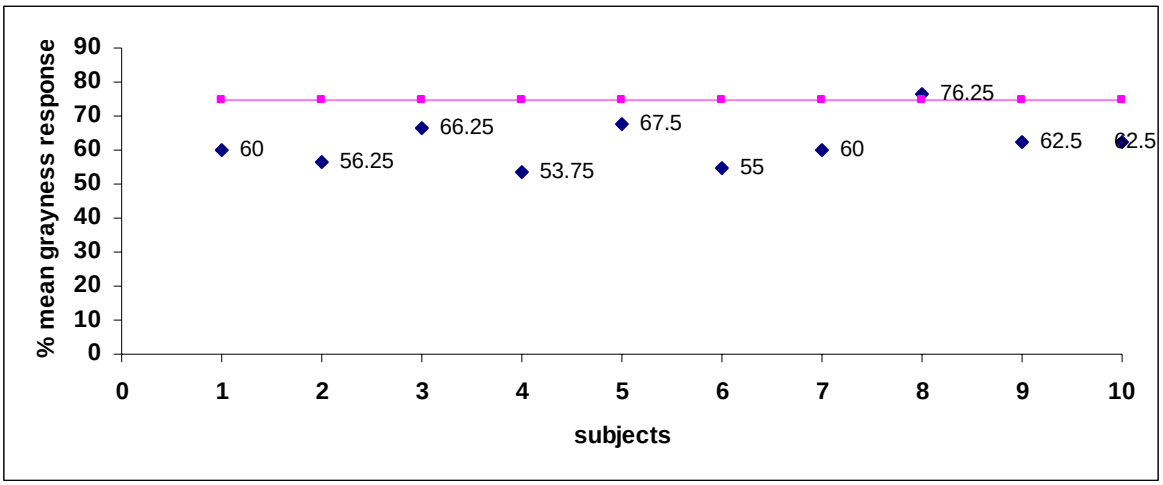

Figure 4.23 Matching results for 75% grayness at motion instant. Initial and terminal luminance values were 100% and 65%. Right motion.

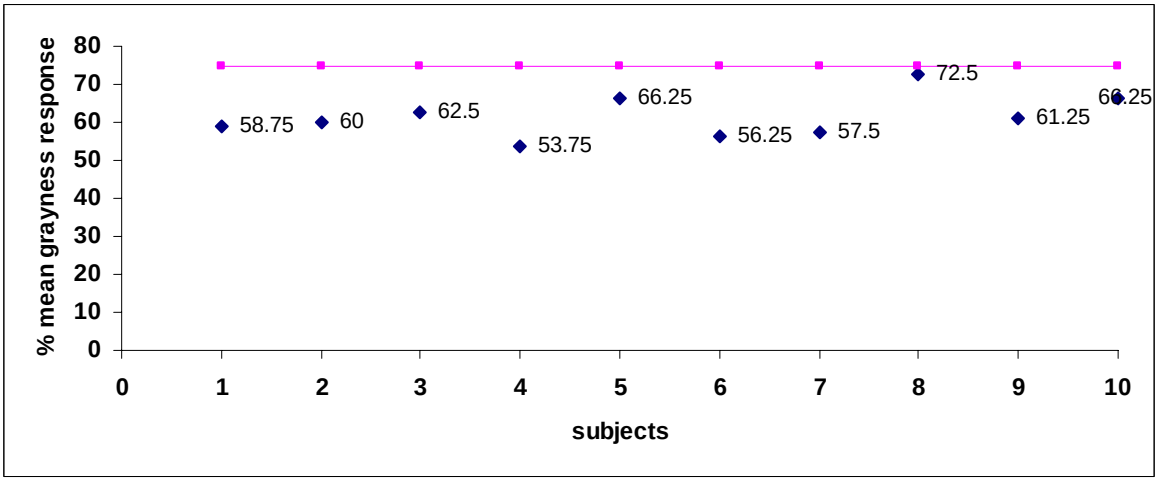

Figure 4.24 Matching results for 75% grayness at motion instant. Initial and terminal luminance values were 100% and 65%. Left motion.

In order to analyze factor effects, 3-way ANOVA was performed in Matlab. The results are given in Table 4.1.

Table 4.1

3-way ANOVA results of ten subjects. There is no interaction between the factors. X1 is the factor for the luminance at the motion instant, X2 is the factor for the motion direction, X3 is the factor for the luminance-change direction.

Analysis of Variance

Source	Sum Sq.	d.f.	Mean Sq.	F	Prob>F
X1	1552.3	2	776.2	23.72	0
X2	7.2	1	7.2	0.22	0.64
X3	23236.2	1	23236.2	710.1	0
X1*X2	0.1	2	0.1	0	0.9981
X1*X3	44.1	2	22.1	0.67	0.5106
X2*X3	34.9	1	34.9	1.07	0.3029
X1*X2*X3	47.6	2	23.8	0.73	0.4844
Error	7460.7	228	32.7		
Total	32383.1	239			

In this table, X1 is the factor for the luminance at the motion instant, X2 is the factor for the motion direction (right/left), X3 is the factor for the luminance-change direction (bright to dim or dim to bright). The ANOVA results show that there is no interaction between the factors. Highly significant main effects were found for X1 and X3. Since there were no interactions and no main effect due to the motion direction, the matching errors were pooled across X2 and were presented in the following figure as a function of X1 with X3 as the parameter.

The experimental results were further analyzed for gender. In order to analyze the gender effect, 1-way ANOVA was performed in Matlab. The percentage errors in % mean grayness responses for female and male subjects were analyzed. It was done for both bright to dim and dim to bright luminance-change directions. The factors for the motion direction and the luminance at motion instant were neglected. The ANOVA results show that there is no main effect and interaction for gender when the luminance-change direction is from bright to dim (p=0.829). On the other hand, when the luminance-change direction is from dim to bright, a significant effect is observed for gender (p=0.0084). 1-way ANOVA was also performed in order to analyze motion direction effect on gender. The ANOVA results show that there is no interaction and no main effect due to the motion direction (p=0.38 for right motion, p= 0.724 for left motion).

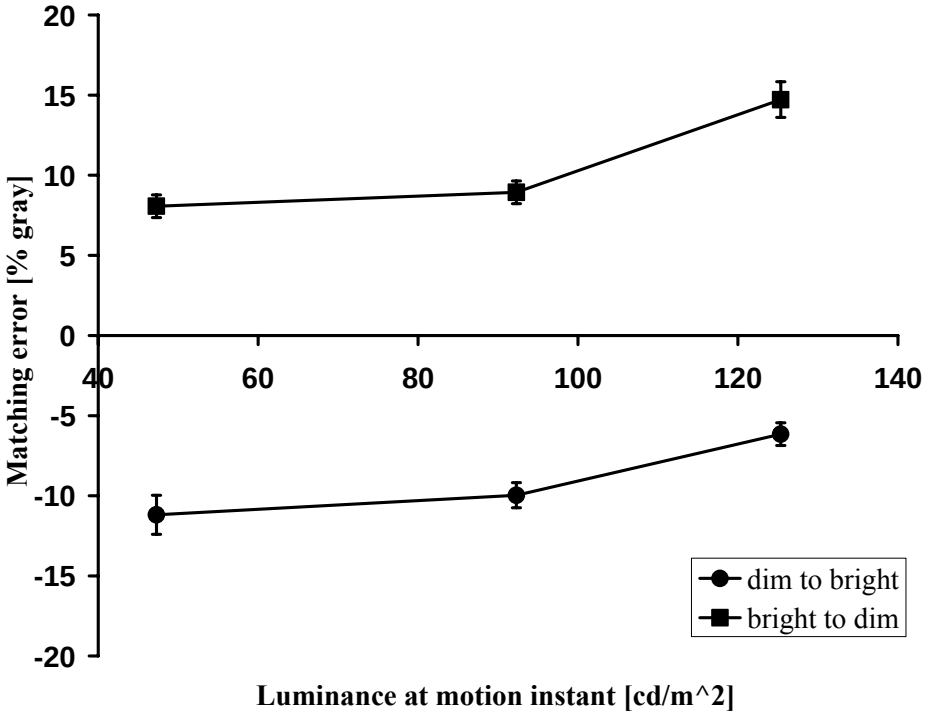

Figure 4.25 A plot of matching errors.

When the luminance-change direction is bright to dim, the matching errors are positive and when the direction is dim to bright, they are negative (Figure 4.25). Positive and negative matching errors indicate the difference between the mean luminance value of the matches and the luminance at motion instant. When the luminance-change direction is reversed, the sign is also reversed and changed from positive to negative or negative to positive. Table 4.2 and Table 4.3 show the values of the matching errors and the standard deviation.

Table 4.2

Matching errors and standard deviation of the mean responses. Luminance-change direction is bright to dim.

Luminance at Motion Instant (cd/m^2)	Bright to Dim Matching Error	Std	SEM
125	14.72	7.04	1.11
92	8.94	4.49	0.71
47	8.07	4.46	0.71

Table 4.3

Matching errors and standard deviation of the mean responses. Luminance-change direction is dim to bright.

Luminance at Motion Instant (cd/m^2)	Dim to Bright Matching Error	Std	SEM
125	-6.16	4.47	0.71
92	-9.97	4.96	0.78
47	-11.19	7.71	1.22

Both positive and negative errors imply that the subjects perceived motion later than luminance, because they matched the luminance of the target at the motion instant to a gray level which appeared later in the luminance-change scale. A plot in time unit is given to show the time-lag magnitude effect (Figure 4.26).

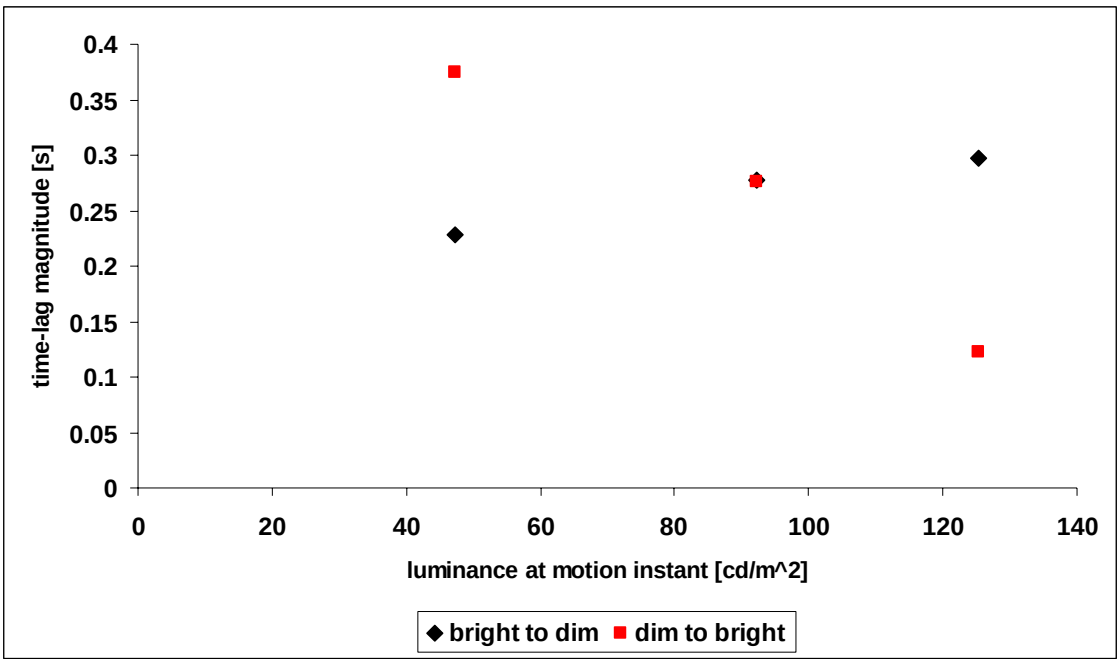

Figure 4.26 Time-lag magnitude effect.

It is also observed that for higher values of luminance at motion instant, absolute-value errors for luminance direction of bright to dim increase and for dim to bright decrease. This may be due a scale compression effect. When luminance change is bright to dim and the motion occurs when the luminance is low, the subject perceives the luminance at motion lower than the veridical value according to the previous paragraph. However, the standard scale has fewer choices at this end of the scale. Similarly, when the luminance change is dim to bright and the motion occurs when the luminance is high, the subject has more limited choices. Therefore, the matching errors are smaller.

There is a motion asymmetry effect at low and high luminance at motion values. For low luminance at motion value, the absolute matching error is higher when luminance changes from dim to bright compared to the error when the change is from bright to dim. On the other hand, for high luminance at motion value, the absolute matching error is lower when luminance changes from dim to bright compared to the error when the change is from bright to dim.

4.2 Computational Results

Two samples of stimuli were used to predict the results. Initial and terminal luminance values were selected to be 153 cd/m^2 and 65 cd/m^2 in the first stimulus type. The luminance of the target at motion instant was 125 cd/m^2. The direction of motion was from left to right. In the second stimulus, initial and terminal luminance values were selected 153 cd/m^2 and 9 cd/m^2. The luminance of the target at motion instant was 47 cd/m^2. The direction of motion was from right to left.

As it is seen from the figures, background luminance (95.66 cd/m^2) was subtracted from every luminance value. In the first stimulus type, the black steps show the decrement of the luminance in the left channel. The red steps show the decrement of the luminance in the right channel. Motion occurs approximately at the time of 0.7 s. The blue curve is the simulated neural activity.

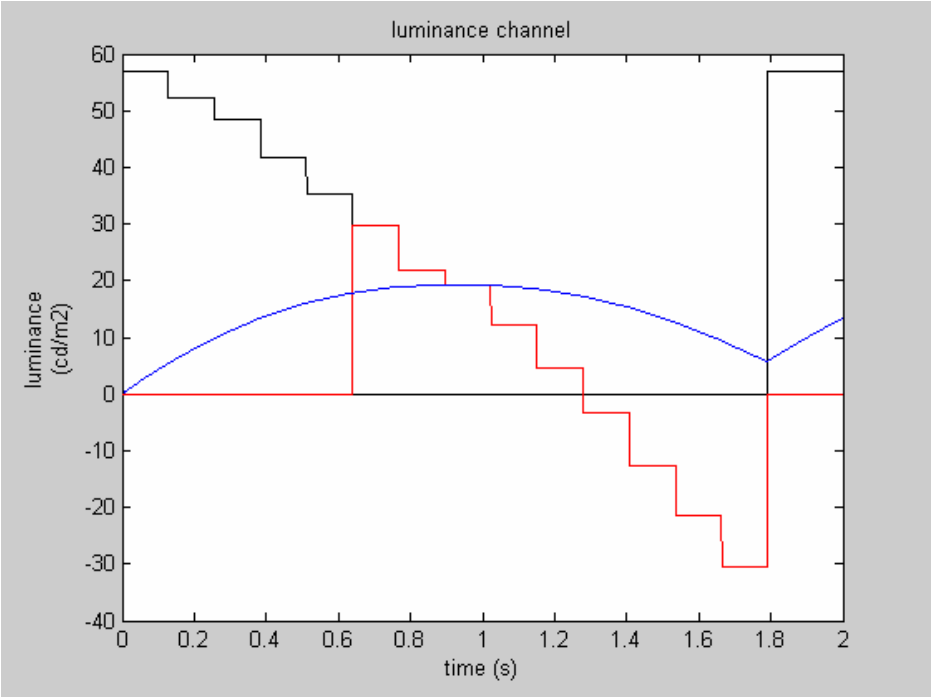

Figure 4.27 The luminance output of the stimulus that has the initial and terminal values of 153 and 65 cd/m^2. The luminance of the target at motion instant is 125 cd/m^2. The direction of motion is from left to right.

As it is seen from the figure above, the neurons are activated and reached to the peak value after motion is occured. This shows a latency between the neural activity of luminance perception and the motion.

In motion channel, there is an increase of neural activity around 0.75 s (Figure 4.28). At this time, the activity is maximum which means that the motion is perceived entirely. The lagged time between the motion and the changing channels can be observed from the graph. The next increase on the right side shows the activity of the repeating stimulus.

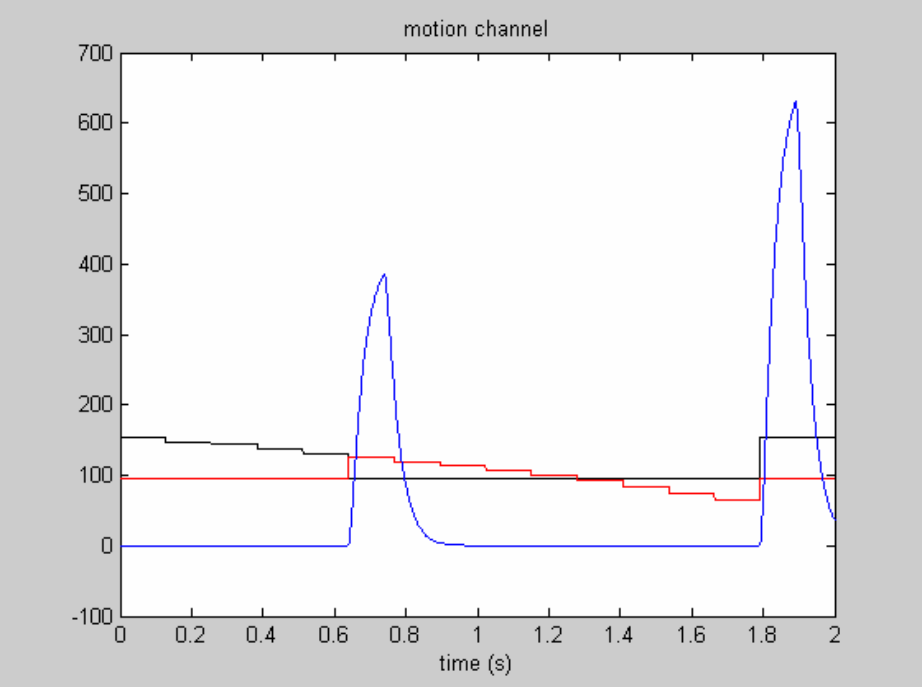

Figure 4.28 The motion output of the stimulus that has the initial and terminal values of 153 and 65 cd/m^2. The luminance of the target at motion instant is 125 cd/m^2. The direction of motion is from left to right.

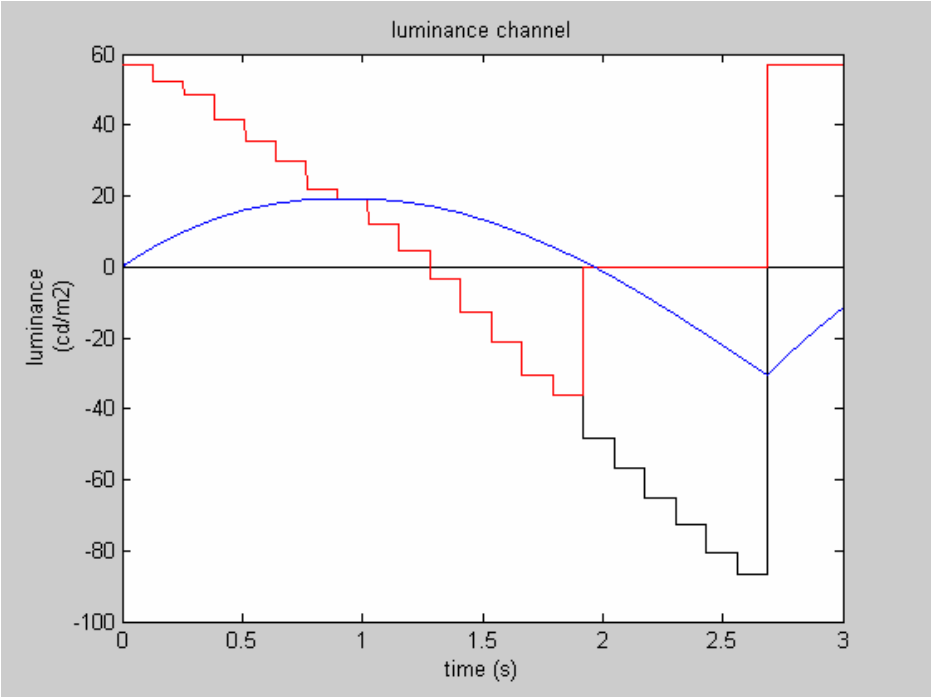

Figure 4.29 The luminance output of the stimulus that has the initial and terminal values of 153 and 9 cd/m^2. The luminance of the target at motion instant is 47 cd/m^2. The direction of motion is from right to left.

For the simulation using the second stimulus, which is shown in Figure 4.29 and Figure 4.30, the red steps show the decrement of the luminance in the right channel. The black steps show the decrement of the luminance in the left channel. Motion occures approximately at the time of 1.8 s. Again the blue curve is the simulated neural activity.

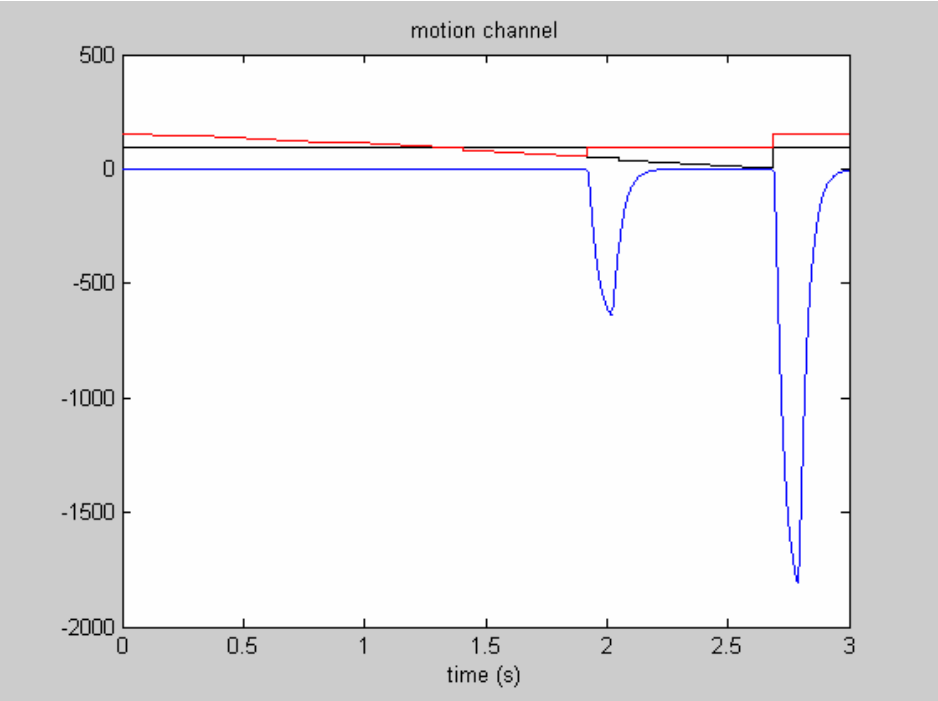

Figure 4.30 The motion output of the stimulus that has the initial and terminal values of 153 and 9 cd/m^2. The luminance of the target at motion instant is 47 cd/m^2. The direction of motion is from right to left.

For both stimulus types, the model predicted that luminance difference should have been perceived about 90 ms after motion. This was calculated by using Weber's constants. It is 0.025 for luminance threshold and 0.44 for motion threshold [14,15]. By using these constants and function analyses, perception times of motion, luminance difference and also the time-lag between these perception times were calculated. 2.5 % decrement of time magnitude from the peak value was taken while calculating the perception time of luminance difference and 44 % decrement of time magnitude from the peak value was taken while calculating the perception time of motion. Then, substraction was done to compare the perception times and to achive the time-lag magnitude. According to these calculations, it was shown that the model did not reproduce the experimental results.

5. DISCUSSION

The visual brain consists of several parallel, functionally specialized processing systems, each having several stages (nodes) which terminate their tasks at different times [1]. The motion system consists of layer 4B of V1, the thick stripes of V2, area V5 and other motion-related areas surrounding it. Each one of these constitutes a node of the motion processing system and the forward connections within this processing system are of the ‘‘like-with-like’’ variety. There are many anatomical opportunities for the nodes comprising the different processing systems to communicate with each other. These connections, referred as lateral connections. The lateral interconnections that anatomically link the different processing systems can be of the like-with-like, the like-with-unlike, or the diffuse variety and are not exclusively hierarchical; they do not appear to bring about cells that integrate different sub-modalities [1].

Anatomical evidence shows that there is no single area to which all the specialized visual areas connect, which would enable it to act as an integrator capable of binding signals coming from all the different visual sources [17]. Each node is therefore only part of a more extensive processing system, which includes, besides subcortical stations, areas in the temporal, parietal, and frontal cortices. The latter areas, too, constitute only parts of the processing system, since they all project to further areas and are reciprocally linked with the earlier visual areas from which they receive input. It is therefore not surprising that there is no terminal station in the cortex, since activity at each node represents, in a sense, a terminal stage of its own specialized process, when it becomes perceptually explicit and acquires a conscious correlate [1]. The communication between nodes that changes the nature of the microconsciousnesses such that they generate a mutually consistent and integrated image in the brain. This brings the grand problem of how the microconsciousnesses are bound together. Indeed, it raises the question of whether they are bound at all, given what appears to be the nonunitary nature of conscious experience.

Most discussions of integration and binding do not give adequate definitions of the terms, assuming them to give one at all. It refers either to the integration or the binding of what is processed by the different processing systems (that is, the binding of different

attributes) or, more commonly, to the binding of the responses of cells within a single processing system [1]. There are two types of binding or integration that differ from each other in physiological implementation and type of neural code used. One of them is generative binding, which is always hierarchical and preconscious. It generates cells with new receptive field properties, is accompanied by receptive field enlargement, and is mediated by a like-with-like, bottom-up input. It combines the activity of two or more cells onto a third cell in a reliable and reproducible fashion, and the response of the third cell depends entirely on the firing of the cells feeding it. The second one is parallel binding. It is the coupling of the activity of cells within a single area or across different areas. Activity at each node has a conscious correlate. Therefore, this binding is postconscious, since it is the microconsciousness generated at a given node of one processing system that is bound to the microconsciousness generated at a given node of another (or the same) processing system. S. Zeki and A. Bartels (1998) hypothesized that mere communication between areas will not result in a microconscious correlate. It is only the cellular activity at the nodes which does so. Therefore, binding must result in a change of the activity at the nodes involved so that altered microconsciousnesses are generated at each. The binding can also be between two groups of cells at a given node, whose activities have a conscious correlates. The parallel binding facilitates figure-ground separation or brings different visual attributes such as color, luminance and motion together through the synchronous or oscillatory firing of cells in different nodes and that this is necessary for generating conscious perception [1].

We are conscious of what we perceive and are not conscious of what we do not perceive and do not perceive what we are not conscious of [18]. The question is whether two visual events which occur together in real time are also perceived simultaneously. One of the previous studies implies that the color processing system reaches its perceptual end point before the motion processing system (Moutoussis & Zeki, 1997). The brain does not necessarily bind together what happens in real time but appears instead to bind the results of the operations undertaken by its different processing systems, which require different amounts of time to complete their tasks [1]. In the sub-second window, the brain therefore misbinds in terms of real time (Moutoussis & Zeki, 1997). What this result also implies is

that there is no central perceptual integrator area that takes into account the different time lags of different systems with regard to real time, before binding their results together.

This thesis was on the synchronicity of perception of luminance difference and motion. It was inspired by Kerzel's study [2]. In Kerzel's study, the stimulus was a 0.16º white (70.4 cd/m^2) filled circle moving on a virtual circle with a radius of 1.8º. The background was dark gray (8.4 cd/m^2). 24 equally spaced lines were pointed radially outward from the center of the circle like the dial of a clock. The lines were 0.18º long and started at 2.39º from the circle center. In the center of the virtual circle, a 0.09º fixation dot was presented. The target rotated clockwise at a velocity of 23.4 r.p.m (2.56 s per rotation). The target appeared at a random position along the trajectory of the circle and rotated randomly between 70º and 230º before it changed its luminance. The target either changed its luminance from white (70.4 cd/m^2) to gray (24.1 cd/m^2) or from white (70.4 cd/m^2) to black (0 cd/m^2). After the change, the target continued to move randomly for 70º to 140º. Observers' task was to indicate where on the targets trajectory the visual change occurred and also adjust the cursor to the position at which the small or large luminance decrement occurred. The angular deviation between the judged position of the luminance change and its actual position was calculated. As a result, Kerzel suggested that the perception of first-order motion and luminance difference were not synchronous events. It was suggested that motion was perceived before the luminance difference. Further, the difference of the time-to-consciousness was larger with a small luminance decrement (116-137 ms) than with a large decrement (37 ms) [2].

In this study, the stimuli were filled squares presented on a mid-gray background. The luminance of the target was incremented or decremented. The stimuli transformed from bright to dim and dim to bright and at a certain luminance value the square shifted sideways. This type of incrementing or decrementing stimuli were chosen instead of moving stimuli in order to test the hypothesis by an alternative method to find out the differences in perception times.

Parvo and magno cells have very different visual sensitivities [3]. Extracellular recordings from parvo cells reveal that these cells are not sensitive to fast movement. On

the other hand, magno cells are very sensitive to movement. Because of their anatomic segregation and different visual sensitivities, parvo and magno cells may be considered to be portions of separate visual pathways. Another feature is the time course of their neural response. Parvo neurons show a sustained response when presented with a long-duration stimulus: the neuron continues to respond to the stimulus as long as it is present. Magnocellular neurons respond in a transient fashion: only brief burst of activity is displayed at stimulus onset and offset [3]. In this study, the continuously incrementing or decrementing stimuli with relatively long durations could activate both the parvo and the magno neurons. In Kerzel's study, the stimuli were entirely processed in the magno system and motion was found to be perceived prior to luminance difference. However, in this study, luminance difference was found to be perceived prior to motion. The differences between the stimuli and the neural systems could be the reasons for the inconsistency between these two studies.

The magno pathway also transmits action potentials faster than the parvo pathway [7]. The magno system may be thought of as a more primitive alerting system. It transmits high temporal frequency information, such as rapid movement. It is more sensitive to large stimuli than spatial details. The magno system alerts us that a visual event has occured. Most visual events that deserve attention are associated with movement. The magno system, being sensitive to high temporal frequencies, detects this movement. The details of the alerting visual event are then analyzed by the parvo system [7].

As mentioned before, the detection of luminance difference and the perception of motion are both known to be the functions of the magno system and the associated parietal areas in the visual cortex because of the fast response characteristics of the magnocellular stream and its high contrast sensitivity [2]. However, motion and luminance are both predominantly processed in the magnocellular pathway, and the associated cortical area MT, the results suggest that these two features are perceived at different times and it may be assumed that the perception of motion and the perception of luminance difference are dissociable events.

In addition, there was a motion asymmetry effect at low and high luminance at motion values. For low luminance at motion value, the absolute matching error is higher when luminance changes from dim to bright compared to the error when the change is from bright to dim. On the other hand, for high luminance at motion value, the absolute matching error is lower when luminance changes from dim to bright compared to the error when the change is from bright to dim. This may be a secondary effect of the scale compression mentioned above. However, in both cases the reported luminance values at motion instant were biased towards the luminance-change direction. This suggested that motion was perceived approximately 200 ms later than luminance difference in the experiments. The time-lag is big enough to be tolerated. However, the stimulus conditions (continuously and successively shown stimuli), the task and the procedure of the experiments could arise these results. The model, however, predicted that luminance difference should have been perceived 90 ms later than motion. Therefore, the model did not reproduce the experimental results.

The experimental results were not consistent with either the model prediction or the experimental results reported in the literature. This inconsistency may also be due to a memory effect. Since the task required to keep luminance information in memory, the output of a plausible luminance channel might have been attenuated over time. Therefore, the subjects might have selected only recently seen luminance values, although the motion was perceived earlier. The computational model may be modified in this respect. The data from the literature may be reinterpreted such that motion effects are kept much stronger in memory than luminance changes without motion. The results of this study showed that the visual brain is a temporal asynchrony in vision and, reflecting the consequence of functional specialization in the time domain. Visual perception is therefore modular. When two visual events (luminance and motion) occur together, they do not have to be integrated for each to be perceived. Mutual integration of activity between different processing nodes is not necessary for the creation of a conscious percept. Activity in each separate processing node generates a microconsciousness for the attribute for which that node is specialized. Consequently, there are several microconsciousnesses such as luminance and motion, corresponding to the activity of cells at different nodes within different processing systems.

6. CONCLUSION

Visual consciousness consists of many, functionally specialized, microconsciousnesses which are spatially and temporally distributed if they are the result of activity at spatially distributed sites (as in the case of luminance and motion). The several, parallel, multinodal, functionally specialized, and autonomous processing systems are also perceptual ones and that activity at each node of each processing-perceptual system can become perceptually explicit. Activity at each node therefore has a microconscious correlate which is functionally specialized and asynchronous with the microconscious correlate generated by that at other nodes [1].

In the present study, it was investigated whether luminance difference and motion are processed synchronously or not. It was hypothesized that if the subjects perceived motion first, they would report luminance values back in time from the instant the motion had occurred. Significant main effects were found due to luminance at motion instant and luminance-change direction. The reported luminance values at motion instant were biased towards the luminance-change direction whether it was bright to dim or dim to bright. This suggested that motion was perceived later than luminance difference. A computational model was used to predict the results of the current experiment. However, experimental results were not consistent with either the model prediction or the experimental results reported in the literature.

Motion and luminance difference are assumed to be perceived asynchronously in both Kerzel's and our studies. On the contrary, in this study, the motion was found to be perceived later than the luminance difference. As the conclusion of all, asynchronous processing of luminance difference and motion was demonstrated in visual perception.

APPENDIX

A.1. LISTING OF SOFTWARE

A.1.1

```
for y=1:24
   S{y}=['avi_',num2str(y),'.avi'];

end

amat=zeros(1,24);

a = randperm(24);
sk = aviread('skala.avi');

amat(1,:)=a;

hfig = figure;
haxis = gca;
set(hfig,'position', get(0,'ScreenSize'))
set(haxis,'units','normalized','position', [0 0 1 1])
set(hfig,'WindowButtonDownFcn','ix=1;')
set(gcf,'Position',[0 0 1024 768])

for f=1:24,


   mov = aviread(S{a(f)});
   ix = 0;

   while ~ix,
      movie(mov,10,1/0.128);
      movie(sk,1,1);
   end

   clear mov

end
```

A.1.2

```
dt = 1e-3;
t = 0:dt:2;
n = length(t);

%load dosya


L1=56.98*ones(1,2001);
L1(129:256)=52.28;
L1(257:384)=48.45;
L1(385:512)=41.69;
L1(513:640)=35.22;
L1(641:1792)=0;

R1=0*ones(1,2001);
R1(641:768)=29.69;
R1(769:896)=21.98;
R1(897:1024)=19.28;
R1(1025:1152)=12.22;
R1(1153:1280)=4.69;
R1(1281:1408)=-3.37;
R1(1409:1536)=-12.78;
R1(1537:1664)=-21.37;
R1(1665:1792)=-30.43;



L2=152.64*ones(1,2001);
L2(129:256)=147.94;
L2(257:384)=144.11;
L2(385:512)=137.35;
L2(513:640)=130.88;
L2(641:1792)=95.66;

R2=95.66*ones(1,2001);
R2(641:768)=125.35;
R2(769:896)=117.64;
R2(897:1024)=114.94;
R2(1025:1152)=107.88;
R2(1153:1280)=100.35;
R2(1281:1408)=92.29;
R2(1409:1536)=82.88;
R2(1537:1664)=74.29;
R2(1665:1792)=65.23;
```

```
% luminance channel

tau_lum = 1.3;
h_lum = (1/tau_lum)*exp(-t/tau_lum);

La = conv(L1,h_lum)*dt;
La = La(1:n);


Ra = conv(R1,h_lum)*dt;
Ra = Ra(1:n);


LO = La + Ra;

figure
plot(t,L1,'k',t,R1,'r',t,LO,'b')
title('luminance channel')


% motion channel

tau_mot1 = 0.008;
h_mot1 = (1/tau_mot1)*exp(-t/tau_mot1);

tau_mot2 = 0.035;
h_mot2 = (1/tau_mot2)*exp(-t/tau_mot2);

Lb = conv(L1,h_mot1)*dt;
Lb = Lb(1:n);
Rb = conv(R1,h_mot1)*dt;
Rb = Rb(1:n);

Lc = conv(Lb,h_mot2)*dt;
Lc = Lc(1:n);
Rc = conv(Rb,h_mot2)*dt;
Rc = Rc(1:n);

Ld = Lb.*Rc;
Rd = Rb.*Lc;

Le = Ld;
Re = Rd;

ta2 = 100;
```

```
for f=ta2:n,
   Le(f)=mean(Ld(f-(ta2-1):f));
   Re(f)=mean(Rd(f-(ta2-1):f));
end

MO = Re - Le;

figure
plot(t,L2,'k',t,R2,'r',t,MO,'b')
title('motion channel')
```

A.1.3

```
dt = 1e-3;
t = 0:dt:3;
n = length(t);

%load dosya


L1=0*ones(1,3001);
L1(1921:2048)=-48.37;
L1(2049:2176)=-56.55;
L1(2177:2304)=-65.31;
L1(2305:2432)=-72.84;
L1(2433:2560)=-80.43;
L1(2561:2688)=-86.72;

R1=56.98*ones(1,3001);
R1(129:256)=52.28;
R1(257:384)=48.45;
R1(385:512)=41.69;
R1(513:640)=35.22;
R1(641:768)=29.69;
R1(769:896)=21.98;
R1(897:1024)=19.28;
R1(1025:1152)=12.22;
R1(1153:1280)=4.69;
R1(1281:1408)=-3.37;
R1(1409:1536)=-12.78;
R1(1537:1664)=-21.37;
R1(1665:1792)=-30.43;
R1(1793:1920)=-36.14;
R1(1921:2688)=0;



L2=95.66*ones(1,3001);
L2(1921:2048)=47.29;
L2(2049:2176)=39.11;
L2(2177:2304)=30.35;
L2(2305:2432)=22.82;
L2(2433:2560)=15.23;
L2(2561:2688)=8.94;
```

```
R2=152.64*ones(1,3001);
R2(129:256)=147.94;
R2(257:384)=144.11;
R2(385:512)=137.35;
R2(513:640)=130.88;
R2(641:768)=125.35;
R2(769:896)=117.64;
R2(897:1024)=114.94;
R2(1025:1152)=107.88;
R2(1153:1280)=100.35;
R2(1281:1408)=92.29;
R2(1409:1536)=82.88;
R2(1537:1664)=74.29;
R2(1665:1792)=65.23;
R2(1793:1920)=59.52;
R2(1921:2688)=95.66;


% luminance channel

tau_lum = 1.3;
h_lum = (1/tau_lum)*exp(-t/tau_lum);

La = conv(L1,h_lum)*dt;
La = La(1:n);


Ra = conv(R1,h_lum)*dt;
Ra = Ra(1:n);



LO = La + Ra;

figure
plot(t,L1,'k',t,R1,'r',t,LO,'b')
title('luminance channel')


% motion channel

tau_mot1 = 0.008;
h_mot1 = (1/tau_mot1)*exp(-t/tau_mot1);

tau_mot2 = 0.035;
h_mot2 = (1/tau_mot2)*exp(-t/tau_mot2);
```

```
Lb = conv(L1,h_mot1)*dt;
Lb = Lb(1:n);
Rb = conv(R1,h_mot1)*dt;
Rb = Rb(1:n);

Lc = conv(Lb,h_mot2)*dt;
Lc = Lc(1:n);
Rc = conv(Rb,h_mot2)*dt;
Rc = Rc(1:n);

Ld = Lb.*Rc;
Rd = Rb.*Lc;

Le = Ld;
Re = Rd;

ta2 = 100;

for f=ta2:n,
   Le(f)=mean(Ld(f-(ta2-1):f));
   Re(f)=mean(Rd(f-(ta2-1):f));
end

MO = Re - Le;

figure
plot(t,L2,'k',t,R2,'r',t,MO,'b')
title('motion channel')
```

REFERENCES

1. Zeki, S., Bartels, A., 'Toward a theory of visual consciousness', *Academic Press*, Consciousness and Cognition 8, pp. 225-259, 1999.

2. Kerzel, D., 'Asynchronous perception of motion and luminance change', *Psychological Research,* Vol. 67, pp. 233-239, 2003.

3. Schwartz, S. H., *Visual Perception*, Appleton & Lange, 1994.

4. Matossian Eye Associates, 2002. Available:
http://www.matossianeye.com/.

5. Bruce, V., Green, P.R., Georgeson M.A., *Visual Perception, 4th ed.,* Psychology Press, 2003.

6. Catalase, 2003. Available:
http://www.catalase.com/retina.gif.

7. Merigan, W.H., Maunsell, J.H.R., 'How parallel are the primate visual pathways?', *Annual Reviews*, Vol. 16, pp. 369-402, 1993.

8. Rheingans, P., Motion and Interaction, Available:
http://www.cs.umbc.edu/~rheingan/SIGGRAPH/motion.intro.pdf.

9. Van Santen, J.P.H., Sperling, G., 'Elaborated Reichardt Detectors', *Optical Society of America*, Vol. 2, No. 2, pp. 300-321, 1985.

10. Burr, C., David, 'Motion perception, elementary mechanisms', MIT Press, pp. 1-4, 2003.

11. Watson, A. B., Ahumada, A. J., 'Model of human visual-motion sensing', *Optical Society of America*, Vol. 2, No. 2, pp. 322-342, 1985.

12. Processing second-order motions with the gradient based motion model, 1999. Available:
http://www.dcs.qmul.ac.uk/~pmco/second.html.

13. The perception of second-order motion and orientation, Available:
http://www.psych.usyd.edu.au/staff/colinc/HTML/second.html.

14. Carreno, F., Zoido, J. M., 'The Weber fraction and asymmetries in luminance thresholds', *Wiley Periodicals*, Vol. 27, No. 5, pp. 330-334, 2001.

15.Lu, Z. L., Sperling, G., 'Contrast gain control in first- and second-order motion perception', *Optical Society of America*, Vol. 13, No. 12, pp. 2305-2318, 1996.

16. McKendrick, A.M., Badcock, D.R., Morgan, W.H., 'Psychophysical measurement of neural adaptation abnormalities in magnocellular and parvocellular pathways in glaucoma', *Investigative Ophthalmology & Visual Science*, Vol. 45, No. 6, pp. 1846-1853, 2004.

17. Bartels, A., Zeki, S., 'The theory of multi-stage integration in the visual brain', *Proceedings of the Royal Society*, pp. 2327-2332, 1998.

18. Zeki, S., ‘Parallel processing, asynchronous perception and a distributed system of consciousness in vision’, *The Neuroscientist*, pp. 365–372, 1998.

19. Zeki, S., Bartels, A., ‘The asynchrony of consciousness’, *Proceedings of the Royal Society,* pp. 1583–1585, 1998.

20. Moutoussis, K., Zeki, S., ‘A direct demonstration of perceptual asynchrony in vision’, *Proceedingsof the Royal Society,* pp. 393–399, 1997.

21. Moutoussis, K., Zeki, S., ‘Functional segregation and temporal hierarchy of the visual perceptive systems’, *Proceedings of the Royal Society,* pp. 1407–1414, 1997.

22. Adelson, E.H., Bergen, J.R., ‘Spatiotemporal energy models for the perception of motion’, *Optical Society of America*, Vol. 2, No. 2, pp. 284-299, 1985.

23. Seiffert, A.E., Somers, D.C., Dale, A.M., Tootell, R.B.H., ‘Functional MRI studies of human visual motion perception: texture, luminance, attention and after-effects’, *Oxford University Press*, pp. 340-349, 2003.

24. Braddick, O. J., ‘Low-level and high-level processes in apparent motion’, *Philosophical Transactions of the Royal Society of London. Series B, Biological Sciences*, Vol. 290, No. 1038, pp. 137-151, 1980.

25. Hock, H. S., Gilroy, L. A., ‘A common mechanism for the perception of first-order and second-order apparent motion’, Vision Research, Vol. 45, pp. 661-675, 2005.

26. Eagleman, D. M., Sejnowski, T. J., ‘Motion integration and postdiction in visual awareness’, *Science*, Vol. 287, pp. 2036-2038, 2000.

27. Kanai, R., Sheth, B. R., Shimojo, S., ‘Dynamical evolution of motion perception’, *Vision Research*, Vol. 47, pp. 937-945, 2007.

28. Burkhardt, D. A., Gottesman, J., Keenan R. M., ‘Sensory latency and reaction time: dependence on contrast polarity and early linearity in human vision’, *Optical Society of America*, Vol. 4., No. 3, pp. 530-539, 1987.

29. Allik, J., Kreegipuu, K., ‘Multiple visual latency’, *American Psychological Society*, Vol. 9, No. 2, pp. 135-138, 1998.

30. Regan, D., *Human Perception of Objects*, Sinauer Associates, Inc., 2000.

31. Schaeffel, F., Processing of Information in the Human Visual System, *Handbook of Machine Vision*, WILEY-VCH Verlag GmbH & Co. KGaA,Weinheim, 2006.

32. Sekuler, R., Watamaniuk, S.N.J., Blake, R., *Perception of Visual Motion, 3rd ed.*, J. Wiley Publishers, 2001.

33. Engel, A. K., Fries, P., Roelfsema, P. R., König, P., Singer, W., ‘Temporal binding, binocular rivalry, and consciousness’, *Consciousness and Cognition*, 1999.

34. Livingstone, M. S., Hubel, D. H., 'Segregation of form, color, movement, and depth: anatomy, physiology, and perception', *Science,*pp. 740-749, 1988.

35. Llina´s, R., Ribary, U., Contreras, D., Pedroarena, C., 'The neuronal basis for consciousness', *Philosophical Transactions of the Royal Society of London,*pp. 1841-1849, 1998.

36. Maunsell, J. H. R., Nealey, T. A., DePriest, D. D., 'Magnocellular and parvocellular contributions to responses in the middle temporal visual area (MT) of the macaque monkey', *Journal of Neuroscience,* pp. 3323-3334, 1990.

37. Singer, W., 'Consciousness and the structure of neuronal representations', *Philosophical Transactions of the Royal Society of London,* pp. 1829-1840, 1998.

38. Stoerig, P., Cowey, A., 'Visual-perception and phenomenal consciousness', *Behavioural Brain Research,* pp. 147-156, 1995.

39. Zeki, S., Watson, J. D. G., Lueck, C. J., Friston, K. J., Kennard, C., Frackowiak, R. S. J., 'A direct demonstration of functional specialization in human visual cortex', *Journal of Neuroscience,* pp. 641-649, 1991.